Study on the pulmonary delivery system of apigenin loaded albumin nanocarriers with antioxidant activity

Papay, Z.E., Kosa, A., Boddi, B., Merchant, Z., Saleem, I.Y., Zariwala, M., Klebovich, I., Somavarapu, S. and Antal, I.

This is an author's accepted manuscript of an article published in the Journal of Aerosol Medicine and Pulmonary Drug Delivery doi:10.1089/jamp.2016.1316.

The final definitive version is available online at:

https://dx.doi.org/10.1089/jamp.2016.1316

JOURNAL OF
Aerosol Medicine
and Pulmonary Drug Delivery

Journal of Aerosol Medicine and Pulmonary Drug Delivery; http://mc.manuscriptcentral.com/aerosol

Study on the pulmonary delivery system of apigenin loaded albumin nanocarriers with antioxidant activity

Journal:	*Journal of Aerosol Medicine and Pulmonary Drug Delivery*
Manuscript ID	JAMP-2016-1316.R2
Manuscript Type:	Original Research
Date Submitted by the Author:	03-Jan-2017
Complete List of Authors:	Papay, Zsofia; Semmelweis University, Department of Pharmaceutics Kosa, Annamaria; Institute of Biology, Eötvös Lóránd University, Department of Plant Anatomy Boddi, Bela; Institute of Biology, Eötvös Lóránd University, Department of Plant Anatomy Merchant, Zahra; University College London School of Pharmacy Saleem, Imran; Liverpool John Moores University, School of Pharmacy & Biomolecular Sciences Zariwala, Mohammed ; University of Westminster Klebovich, Imre; Semmelweis University, Department of Pharmaceutics Somavarapu, Satyanarayana ; University College London School of Pharmacy Antal, Istvan; Semmelweis Egyetem, Department of Pharmaceutics
Keyword:	Aerosol Distribution, inhaled therapy, Modeling
Manuscript Keywords (Search Terms):	flavonoid, apigenin, albumin nanoparticles

Study on the pulmonary delivery system of apigenin loaded albumin nanocarriers with antioxidant activity

Zsófia Edit Pápay[1], Annamária Kósa, PhD[2], Béla Böddi, PhD [2], Zahra Merchant[3], Imran Y Saleem, PhD [4], Mohammed Gulrez Zariwala, PhD[5], Imre Klebovich, PhD [1], Satyanarayana Somavarapu, PhD [3*], István Antal, PhD [1*]

[1] Department of Pharmaceutics, Semmelweis University, Hőgyes E. Street 7-9, H-1092 Budapest, Hungary

[2] Department of Plant Anatomy, Institute of Biology, Eötvös Lóránd University, Pázmány Péter Street 1/C, Budapest, Hungary

[3] Department of Pharmaceutics, UCL School of Pharmacy, 29-39 Brunswick Square, London WC1N 1AX, United Kingdom

[4] Formulation and Drug Delivery Research, School of Pharmacy and Biomolecular Sciences, Liverpool John Moores University, Liverpool, United Kingdom

[5] Department of Biomedical Science, Faculty of Science and Technology, University of Westminster, 115 New Cavendish Street, London, W1W 6UW, United Kingdom

* To whom correspondence should be addressed:

antal.istvan@pharma.semmelweis-univ.hu

Department of Pharmaceutics

Semmelweis University

Hőgyes E. Street 7-9,

H-1092 Budapest, Hungary

Tel/Fax: +3612017-0914; Tel.: +361476-3600/53066, 53087

Running title:

Albumin-Apigenin Nanoparticles against Lung Injury

Study on the pulmonary delivery system of apigenin loaded albumin nanocarriers with antioxidant activity

Zsófia Edit Pápay[1], Annamária Kósa, PhD[2], Béla Böddi, PhD [2], Zahra Merchant[3], Imran Y Saleem, PhD [4], Mohammed Gulrez Zariwala, PhD[5], Imre Klebovich, PhD [1], Satyanarayana Somavarapu, PhD [3*], István Antal, PhD [1*]

[1] Department of Pharmaceutics, Semmelweis University, Hőgyes E. Street 7-9, H-1092 Budapest, Hungary

[2] Department of Plant Anatomy, Institute of Biology, Eötvös Lóránd University, Pázmány Péter Street 1/C, Budapest, Hungary

[3] Department of Pharmaceutics, UCL School of Pharmacy, 29-39 Brunswick Square, London WC1N 1AX, United Kingdom

[4] Formulation and Drug Delivery Research, School of Pharmacy and Biomolecular Sciences, Liverpool John Moores University, Liverpool, United Kingdom

[5] Department of Biomedical Science, Faculty of Science and Technology, University of Westminster, 115 New Cavendish Street, London, W1W 6UW, United Kingdom

* To whom correspondence should be addressed:

antal.istvan@pharma.semmelweis-univ.hu

Department of Pharmaceutics

Semmelweis University

Hőgyes E. Street 7-9,

H-1092 Budapest, Hungary

Tel/Fax: +3612017-0914; Tel.: +361476-3600/53066, 53087

Running title:

Albumin-Apigenin Nanoparticles against Lung Injury

ABSTRACT

Background: Respiratory diseases are mainly derived from acute and chronic inflammation of the alveoli and bronchi. The pathophysiological mechanisms of pulmonary inflammation mainly arise from oxidative damage that could ultimately lead to acute lung injury (ALI). Apigenin (Api) is a natural polyphenol with prominent antioxidant and anti-inflammatory properties in the lung. Inhalable formulations consist of nanoparticles (NPs) have several advantages over other administration routes therefore this study investigated the application of apigenin loaded bovine serum albumin nanoparticles (BSA-Api-NPs) for pulmonary delivery.

Methods: Dry powder formulations of BSA-Api-NPs were prepared by spray drying and characterized by laser diffraction particle sizing, scanning electron microscopy, differential scanning calorimetry and powder X-ray diffraction. The influence of dispersibility enhancers (lactose monohydrate and L-leucine) on the *in vitro* aerosol deposition using a next generation impactor (NGI) was investigated in comparison to excipient-free formulation. The dissolution of Api was determined in simulated lung fluid by using Franz cell apparatus. The antioxidant activity was determined by 2,2-Diphenyl-1-picrylhydrazyl (DPPH$^{\bullet}$) free radical scavenging assay.

Results: The encapsulation efficiency and the drug loading was measured to be 82.61 ± 4.56% and 7.51 ± 0.415%. The optimized spray drying conditions were suitable to produce particles with low residual moisture content. The spray dried BSA-Api-NPs possessed good the aerodynamic properties due to small and wrinkled particles with low mass median aerodynamic diameter, high emitted dose and fine particle fraction. The aerodynamic properties was enhanced by leucine and decreased by lactose, however, the dissolution was reversely affected. The DPPH$^{\bullet}$ assay confirmed that the antioxidant activity of encapsulated Api was preserved.

Conclusion: This study provides evidence to support that albumin nanoparticles are suitable carriers of Api and the use of traditional or novel excipients should be taken into consideration. The developed BSA-Api-NPs is a novel delivery system against lung injury with potential antioxidant activity.

Keywords: aerosol distribution, inhaled therapy, modeling

1. INTRODUCTION

Respiratory diseases are thought to be mainly derived from acute and chronic inflammation of the alveoli and the bronchi. The pathophysiological mechanisms of pulmonary inflammation arise from several factors, including oxidative damage due to cytotoxic mediators that may ultimately lead to acute lung injury (ALI), acute respiratory distress syndrome (ARDS) and cancer[1]. A growing body of scientific data suggests that natural occurring compounds possess preventive and therapeutic properties with inherent low toxicity[2]. Among phytochemicals, apigenin (Api, **Figure 1**) is a promising candidate as a therapeutic agent, mainly due to its antioxidant and anti-inflammatory properties[3-6]. It has been demonstrated that Api has protective effects against bleomycin-induced lung fibrosis in rats which is associated with its antioxidant and anti-inflammatory capacities[7]. Another study provided evidence that Api has was able to decrease oxidative stress and inflammation on paraquat-induced ALI in mice[8] and reduced the pathological alterations of pulmonary tissue in acute pancreatitis associated ALI, therefore suggesting protection in the lung[9]. Furthermore, Api has anti-inflammatory effect owing to significant inhibition of pro-inflammatory cytokines, activator protein (AP-1) and cyclooxygenase-2 (COX-2) in human pulmonary epithelial cells[10] and in mice as well[11]. However, Api's has low water solubility (2.16 μg/ml at pH 7.5) and therefore it was recently classified as BCS (Biopharmaceutical Classification System) II. drug[12].

Encapsulation and delivery of phytoconstituents with health effects has attracted much attention in recent years. Developing a suitable carrier system is essential to improve the overall activity and reduce the possible toxicity of these agents[13]. Among the potential carrier systems, serum albumin nanoparticles have notable advantages including biodegradability, non-antigenicity and cell-targeting ability[14,15]. Moreover, albumin provide exceptional ligand binding capacity for various drugs owing to three homologous domains with two separate

helical subdomains[16]. Studies reported the successful incorporation of flavonoids into albumin nanoparticles that can improve their stability[17] and antitumor activity[18].

Pulmonary delivery of pharmacologically active ingredients are extensively studied due to prominent advantages over other delivery routes of administration[19]. The lungs have a large surface area, limited enzymatic activity and high permeability therefore drugs can be delivered either locally for the treatment of respiratory diseases or systematically in order to e.g. avoid first pass metabolism[20]. Dry Powder Inhaler (DPI) products offer precise and reproducible delivery of fine drug particle fraction to the deep lung and recent studies have proved that these are more cost effective than other products[21]. This non-invasive delivery route could be suitable for poorly water soluble drugs in nanoparticles with increased solubility[22]. It is also well recognized that nanoparticles have benefits over other carriers in the micron scale such as controlled drug release, avoiding mucociliary clearance and improve deposition[23, 24]. Albumin is naturally present in the body, as well as in the lung epithelium[24], moreover, the body can absorb proteins into the bloodstream by transcytosis which occurs deep in the lung and allows drug molecules to pass through cell membrane[25]. Therefore the presence of BSA in the nanoparticle system increases membrane permeability, may facilitate epithelial cell uptake and translocation through the alveo-capillary barrier of the lung[26]. It was proved that albumin nanoparticles have high biocompatibility in a wide dose range and remained longer in the lungs with low systemic exposure[24]. Thus encapsulation of apigenin into albumin nanoparticles would enhance its solubility and distribution in the lung. However, the formulation of dry powders with optimal aerodynamic properties for pulmonary drug delivery is challenging. Spray drying is a technique for manufacturing respirable dry powders in one step. During the process, the liquid phase is atomized into droplets that dry rapidly in the drying chamber due to the compressed air. The process conditions like heat, flow rate, aspiration rate and pump rate also determine the quality of the product. The thermal

degradation caused by overheating can be avoided by the rapid evaporation of the solvent[27]. Hence, it is suitable for drying colloidal systems resulting in uniform particle morphology. Nanoparticle delivery systems targeted to the lungs offer several advantages such as sustained release, increased local drug concentration and targeted site of action[28]. Moreover, improved drug solubility, uniform dose distribution and fewer side effects can be achieved, compared to conventional dry powders. In general, respirable nanoparticles are embedded in microparticles in aerodynamic size range [26].

The aim of this work was to develop a novel dry powder formulation against ALI caused by oxidative stress. The prepared albumin nanoparticles were characterized in terms of size, zeta potential and drug loading, additionally the fluorescence properties were investigated. Following this, the nanoparticles were spray dried with two types of excipients, namely a traditional lactose monohydrate and a novel amino acid, L-leucine. *In vitro* aerosol deposition patterns were determined in comparison to excipient-free formulation using a next generation impactor (NGI) and dissolution test was performed in simulated lung fluid by using Franz cell apparatus. Laser diffraction particle sizing, morphology and residual moisture content were measured along with the antioxidant activity.

2. MATERIALS AND METHODS

MATERIALS

Apigenin (Api) was purchased from (purity > 99%) Hangzhou Dadyangchem Co., Ltd. (China). Bovine serum albumin powder (BSA, purity ≥ 98%), L-leucine, analytical grade chloroform, acetonitrile and trifluoroacetic acid (TFA) were obtained from Sigma Aldrich Ltd. (Dorset, UK). Lactohale® LH 230 was supplied by Friesland Foods Domo (Amersfoort, The Netherlands). 2,2-Diphenyl-1-picrylhydrazyl (DPPH˙) free radical was purchased from Sigma-Aldrich (Darmstadt, Germany). For the solubility and drug release study, PBS buffer was purchased (Sigma Aldrich Ltd., Dorset, UK) and simulated lung fluid modified with

0.02% (w/v) (mSLF) was prepared. All of the materials for the mSLF were purchased from Sigma Aldrich Ltd. (Dorset, UK).

METHODS

2.1. Preparation of BSA-NPs

BSA nanoparticles were prepared using a nanoparticle albumin bound technology with minor modifications[29]. Briefly, 1000 mg of BSA was dissolved in 50 ml of distilled water saturated with chloroform. Separately, 100 mg of Api was dissolved in 3 ml of chloroform saturated with water and ultrasonicated for 10 minutes. These two solutions were mixed and ultrasonicated for 20 minutes with a probe-type sonicator (MSE Soniprep 150 Ultrasonic Processor, MSE Ltd., London, UK) on ice. After homogenization, the chloroform was evaporated by rotary evaporator (Rotavapor® R-10, BÜCHI Labortechnik AG, Flawil, Switzerland) at 25°C for 15 minutes. The obtained nanoparticles were filtered through filter paper (0.45µm, Ficher Scientific Ltd., Loughborough, UK) and further spray dried.

2.2. Characterization of BSA-Api-NPs

2.2.1. Particle size and zeta potential analysis

The average particle size and polydispersity index (PDI) were determined by dynamic light scattering (DLS) using Zetasizer Nano ZS instrument (Malvern Instruments Ltd., Worcestershire, UK). Zeta potential of the particles was quantified with laser doppler velocimetry (LDV) using the same instrument. All measurements were performed in triplicate (n=3) at 25 °C and presented as mean ± standard deviation (SD).

2.2.2. Determination of drug loading and encapsulation efficiency

To determine the amount of Api, 1 ml sample from the BSA-Api formulation was withdrawn and the apigenin content was determined in mg/ml by adding 5 ml of dimethyl sulfoxide and methanol (DMSO:MeOH, 50:50% v/v) and sonicated for 10 minutes. The exact concentrations were determined after filtration (0.22 µm) by HPLC 1260 (Agilent

Technologies Inc., Santa Clara, USA) using reverse-phase C_{18} column (Phenomenex®, 250x4.6 mm, 4µm) as the stationary phase. The temperature was set to 25 °C. The mobile phase consisted of 40% acetonitrile and 60% water containing 0.1% (v/v) TFA. The system was run isocratically at the flow rate of 1.2 ml/min and the Api was detected at 340 nm (t_R = 8.3). The injection volume was set to 10 µl. A calibration curve was conducted by diluting stock solution (0.1 mg/ml) with R^2 value of 0.999.

The drug loading efficiency (DL, %) and encapsulation efficiency (EE, %) were calculated according to the equations (Eq. 1. and 2.), comparing the encapsulated Api content (mg/ml, $W_{encapsulated}$) to total nanoparticle system which means the weighted amount of BSA and Api together (mg/ml, W_{total}) and the amount of Api (mg/ml, $W_{theoretical}$) used in the formulations.

$$DL\ (\%) = \frac{W_{encapsulated}}{W_{total}} \times 100 \qquad \text{Eq.1.}$$

$$EE\ (\%) = \frac{W_{encapsulated}}{W_{theoretical}} \times 100 \qquad \text{Eq.2.}$$

2.2.3. Fluorescence spectroscopy

The fluorescence emission spectra of BSA and BSA-Api-NPs were measured with Jobin Yvon-Horiba Fluoromax-3 (Paris, France) spectrofluorometer. The samples which contained the nanoparticles were diluted 10 times and the fluorescence emission spectra were recorded between 300 and 450 nm at 25 °C where the excitation wavelength was set to 285 nm. The data collection frequency was 0.5 nm and the integration time was 0.2 s. The excitation slit was set at a bandpass width of 2 nm and the emission slit at 5 nm. Each spectrum was recorded three times and the mean values were calculated automatically. The SPSERV V3.14 software (© Csaba Bagyinka, Institute of Biophysics, Biological Research Center of the Hungarian Academy of Sciences, Szeged, Hungary) was used for baseline correction, for five point linear smoothing and for the correction to the wavelength-dependent

sensitivity changes of the spectrofluorometer. The subtraction of the Raman band at 390 nm was performed.

To obtain the three-dimensional projections and contour maps of fluorescence spectra of the samples, the fluorescence emission were recorded from 265 to 450 nm using different excitation wavelengths from 250 to 310 nm with 10 nm-steps with the same instrument mentioned above. All emission scan ranges were set to start at least 15 nm away from the corresponding excitation wavelengths. Other settings were similar as described above. Each spectrum was recorded three times and the mean values were calculated automatically. The three-dimensional fluorescence spectra were visualized with the software SURFER Version 10 (Golden Software, Inc., Colorado, USA). Spectra were combined together into a three dimensional surface data set with axes of excitation and emission wavelengths and fluorescence intensity. Data were also converted into two dimensional contour maps.

2.3. Spray drying of BSA-Api-NPs

Spray drying of the BSA-Api formulations without excipient and in the presence of lactose monohydrate (50%, w/w) and L-leucine (9%, w/w) were carried out in a Büchi 290 Mini Spray Dryer (BÜCHI Labortechnik AG, Flawil, Switzerland). The concentration of the excipients were with respect to the mass of the nanoparticles before spray drying. The following operating conditions were used based on pilot experiments: inlet temperature 120 °C, approximate outlet temperature 65-70 °C, the drying airflow 600 L/h, aspiration rate 100% (35 m^3/h), the nozzle diameter was a 0.1 mm and the liquid feed rate was set to 5 ml/min. Each preparation were carried out in triplicate. Following spray drying, the powders were collected from the lower part of the cyclone and the collecting vessel, stored in tightly sealed glass vials under vacuum at room temperature.

2.4. Characterization of spray-dried BSA-Api-NPs

2.4.1. Determination of residual moisture

The moisture content of the spray-dried powders was measured by using Karl Fischer titration (Metrohm 758 KFD Titirino, Metrohm AG, Lichtenstein, Switzerland). For that purpose approx. 100 mg of the product was analysed and the instrument was previously calibrated with 10 µl distilled water. The evaluation was conducted in triplicate and the standard deviation calculated.

2.4.2. Fourier-Transform Infrared Spectroscopy (FT-IR)

FT-IR spectra of BSA-Api spray-dried samples were evaluated using a PerkinElmer Spectrum 100 FT-IR spectrometer equipped with Universal ATR (Attenuated Total Reflectance) accessory (PerkinElmer Inc., Waltham, USA). Approximately 2 mg of the solid samples were placed between the plate and the probe. The spectra were recorded with 3 scans, in the frequency range between 4000-600 cm^{-1} and with a resolution of 4 cm^{-1} at room temperature. The data were analyzed using the PerkinElmer Spectrum Express software.

2.4.3. X-ray powder diffraction (XRPD)

XRPD diffractograms were obtained using an X-ray diffractometer (MiniFlex600 Rigaku Corporation, Tokyo, Japan). The analyses were performed at room temperature and the samples were scanned from 2° to 40° 2θ using a scanning speed of 2°/min with a step size of 0.05°.

2.4.4. Differential scanning calorimetry (DSC) analysis

The spray-dried formulations were characterized by DSC (DSC Q2000 module; TA Instruments, New Castle, UK) which was calibrated using indium. Samples (3-5 mg) were weighed accurately and analyzed in sealed and pierced aluminium hermetic pans (TA Instruments). The pans were equilibrated at 25 °C and then heated at a rate of 10 °C/min in a range of 50–400 °C.

2.4.5. Aerosol particle size analysis and redispersibility in water

The particle size analysis was conducted by using a Sympatec HELOS laser diffractometer (Sympatec GmbH System-Partikel-Technik, Clausthal-Zellerfeld, Germany). The powders were dispersed by compressed air (4-5 bar) into the measuring zone of the laser beam. The optical lens (0.45–87.5 µm size range) focused onto the detector to collect the diffracted light for calculation of size distribution. The values of 10th (D_{10}), 50th (D_{50}) and 90th (D_{90}) of the cumulative particle size distribution are generated. Samples were measured in triplicate.

The particle size was also determined after spray drying. 5 mg dry powder of each formulation could be easily redispersed in 5 ml distilled water and the particle size was determined without any further dilution by the above mentioned Zetasizer Nano ZS instrument (Malvern Instruments Ltd., Worcestershire, UK).

2.4.6. Solubility and Drug release studies of BSA-Api formulations

The solubility of BSA-Api formulations were determined in PBS buffer (pH 7.4) and in modified simulated lung fluid (mSLF, pH 7.4) which contained 0.02% (w/v) DPPC was prepared according to Son and McConville[30]. 50 mg of samples of spray dried powders were added to 100 mL solvent and shaken (150 rpm) for 2 h at 37 °C. At predetermined time points 1 mL of samples were taken from each dissolution media and replaced with the same volume of fresh medium. All of the samples were diluted with 1 ml methanol and filtered with Amicon® Ultra Centrifugal filters (30K, Merck Millipore, Merck KGaA, Germany) prior to the injection and the amount of apigenin was determined by HPLC-UV method.

The *in vitro* drug release study of the three formulations were conducted with Franz cell apparatus. The mSLF was used as dissolution media and 0.45 µm cellulose acetate membrane filter (Sartorius AG, Goettingen, Germany) was applied. Briefly, an accurately weighed amount (10 mg) of spray dried nanoparticles of each formulations were scattered onto the membrane which was previously wetted with the dissolution media for 1 hour. 1 ml of

samples were withdrawn at various time intervals for 5 hours and replaced with fresh dissolution medium. After the measurement, membrane was rinsed with 2 ml of MeOH and the drug content of the possibly remained powders was determined. The sample preparation and the measurement was the same as mentioned above. The cumulative amount of apigenin release over the time was plotted for each formulations. All measurements were performed in triplicate.

2.4.7. Aerosol delivery of BSA-Api formulations

In vitro aerodynamic performance of BSA-Api formulations was assessed using the next generation impactor (NGI; Copley Scientific Ltd., Nottingham, UK), connected sequentially to a low capacity pump via the critical flow controller (Model LCP5; Copley Scientific Ltd., Nottingham, UK). During the measurement the pump was operated at air flow rate of 60 L/min for 4 s. The 3x10 mg powder aliquots from each formulation were loaded manually into gelatine capsules (size 3) and placed into the inhaler device (Cyclohaler®, Pharmachemie, London, UK) which was connected to the NGI via an airtight rubber adaptor and a stainless steel USP throat. The NGI stages were assembled with an induction port, a pre-separator and a filter was placed in the final stage. Prior to the impaction, the collection plates were uniformly coated with 1 ml of 1% silicone oil in N-hexane solution and allowed to dry leaving a thin film of silicone oil on the plate surface in order to prevent the re-entrainment of the particles and the pre-separator was filled with 15 ml DMSO:MeOH (50:50%, v/v) mixture. After the deposition of the powders in the NGI, the amount of each formulation was cumulatively collected onto silicone-coated plates for each of the stages. The inhaler, mouth piece, induction port, pre-separator and the collection plates were rinsed with DMSO:MeOH (50:50%, v/v) mixture, collected in volumetric flasks (10 or 25 ml) and made up to volume. The samples were determined by using HPLC method as described previously. To characterize the aerosol performance the following parameters were calculated based on

the drug mass of each fraction: emitted dose (ED, %): the percentage of the entire dose depositing from the mouthpiece of the inhaler device and recovered dose (RD, %): the total recovered drug mass. The fine particle fraction (FPF, <4.46 μm) is defined as the percentage of the emitted dose which deposited from the Stage 2-7 and the micro orifice-collector (MOC). The mass median aerodynamic diameter (MMAD) and geometric standard deviation (GSD) were calculated from the inverse of the standard normal cumulative mass distribution against the natural logarithm of the effective cut-off diameter of the respective stages. All measurements were carried out in triplicate.

2.4.8. Particle morphology

Morphology of Api powder and spray-died nanoparticles was examined using scanning electron microscopy (SEM) analysis. The dry powder of the formulations was placed on the sample holder using double adhesive tape and gold coating (~20 nm thickness) was applied. Examinations were performed by FEI Inspect^{TM} S50 (Hillsboro, Oregon, USA) scanning electron microscope at 20.00 kV accelerating voltage. Original magnifications were 8000x, 10,000x and 20,000 x with accuracy of ± 2%.

2.5. Antioxidant activity

The antioxidant activities of the prepared spray-dried formulations were compared to the pure Api in order to investigate the effectiveness of the formulation. The free radical scavenging activity was measured by using DPPH$^{\bullet}$ method as described previously[31] with slight modifications. Methanolic stock solution of 0.1 mM DPPH$^{\bullet}$ reagent was freshly prepared and protected from light. Standard curve was plotted between the DPPH$^{\bullet}$ concentration (0.01-0.1 mM) and absorbance, the linear relationship was calculated graphically. 1 ml of MeOH was added to the BSA-Api-NPs and the concentration of Api were the same in each sample for the comparability. Thereafter 2 ml of 0.06 mM DPPH$^{\bullet}$ reagent was added to the samples, vortex mixed for 10 seconds and protected from light. The

absorbance at 517 nm was determined with spectrophotometer (UV-Vis spectrophotometer, Metertech SP-8001, Metertech Inc., Taipei, Taiwan) in every 15 minutes until the steady state (when no further discoloration could be observed). The addition of samples resulted decrease in the absorbance of DPPH˙ due to the scavenging activity of Api. The exact concentration of the free radical was calculated using the standard curve. To calculate the inhibition of the free radical DPPH˙ the following equation (Eq.3.) was used:

$$I\ (\%) = \frac{A_0 - A_S}{A_0} \times 100 \qquad \text{Eq.3.}$$

Where I (%) is the inhibition in percent, A_0 is the absorbance of the DPPH˙ solution and A_s is the absorbance of the sample. All measurements were carried out triplicate and the data were expressed as the mean value ± SD.

3. RESULTS AND DISCUSSION

3.1. Characterization of BSA-Api-NPs

3.1.1. Size, zeta potential and drug content

Albumin is a natural protein that has been widely used as a macromolecular carrier for many drugs with low water solubility. Several techniques are available to prepare albumin nanoparticles including desolvation (coacervation), nab (nanoparticle albumin bound)-technology and self-assembly[14] . In this study the BSA-Api-NPs were prepared by using modified nab-technology with ultrasonication. The achieved mean particle size of three samples was 376 ± 7.824 nm with a polydispersity index of 0.285 ± 0.01. The size of albumin NPs less than 500 nm could localize effectively in the lung. The PDI value indicated narrow particle size distribution and the uniformity of the nanoparticles. The zeta potential was -19.20 ± 0.818 mV. The higher the zeta potential, the more stable the formulation is, less aggregation occurs[32]. The EE was determined to be 82.61 ± 4.56% and the DL was 7.51 ± 0.415%. Therefore these results confirmed the high encapsulation efficiency of apigenin by BSA-NPs and it can be attractive tool in encapsulation flavonoids for delivery. Similar data were found

in the literature when encapsulating flavonoids into albumin nanoparticles. Human serum albumin-bound curcumin nanoparticles resulted 7.2 ± 2.5% loading efficiency[33] and scutellarin-loaded bovine serum albumin nanoparticles possess 64.46% EE and 6.73% DL[34].

3.1.2. Fluorescence spectroscopy

The phenomenon of fluorescence quenching can result from various inter and intramolecular interactions such as energy transfer, conformational changes, complex formation (static quenching) or collisional interaction (dynamic quenching). During static quenching the quencher forms a stable non-fluorescent complex with the fluorophore, however, during dynamic quenching it collides with the fluorophore and facilitates non-radiative transitions to the ground state[35]. Therefore quenching of the intrinsic fluorescence of the two tryptophan residues (Trp-134 and Trp-212) of BSA can offer information about the changes in molecular microenvironment of these fluorophores, located in domain I and II, respectively. Trp-134 residue is located close to the protein surface in a hydrophilic environment, while Trp-212 is within a protein pocket which is hydrophobic (subdomain II A). The Trp-214 in human serum albumin (HSA) is located similarly to Trp-212 in BSA[36-38]. The quenching effect of Api on fluorescence intensity of serum albumins (BSA and HSA) has been studied previously[36, 39-42] but there is no data related to its behavior in a nanoparticulate system. Studies have shown that the increasing concentration of Api resulted in a decrease in the fluorescence emission intensity of serum albumin solutions. This was mainly attributed to complex formation (static quenching), however, it could be dynamic quenching at higher Api concentrations[42]. Nevertheless, all studies concluded that Api most likely binds to the sub-domain IIA of Site I side with electrostatic and hydrophobic interactions, through which H-bonds and non-radiative energy transfer can occur. The binding could affect the conformation of Trp micro-region but the secondary structure of serum albumin is not altered[36, 39, 41].

However, the pH and ionic concentrations (e.g. NaCl) can affect the fluorescence quenching on the binding parameters of apigenin to BSA[43].

Figure 2 demonstrates the fluorescence emission spectra of BSA solution, BSA-NPs and BSA-Api-NPs. The fluorescence intensity of BSA-NPs decreased slightly compared to BSA solution with no obvious shift of the maximum position at 350 nm. It was probably due to the conformational changes of the protein. The significantly lower emission intensity of BSA-Api-NPs indicates that Api could quench the fluorescence of BSA which is also reflected on the 3D projections (**Figure 3**). All of these findings indicate that Api binds to the Trp region (Trp-212, subdomain II A) but the spectral maximum was not affected therefore hydrophobicity and polarity of the fluorophore residues are not altered. It was concluded that Api can be bound to the Trp region of serum albumin nanoparticles similarly to the solutions.

3.2. Characterization of spray-dried BSA-Api-NPs

3.2.1. Determination of residual moisture

Moisture content is mainly influenced by the spray drying conditions. Increased heat energy availability provided by regulating inlet air temperature and aspirator capacity allows more efficient drying, thus resulting in the lower moisture content demonstrated. However, degradation of heat sensitive materials such as proteins may occur; therefore inlet air temperature should be kept below 120 °C[44]. The water content is also affected by the type of excipients and the ratio with the nanoparticles[45]. Moisture content is an important factor that can significantly influence the aerodynamic properties of aerosols. It can change the surface of particles, promote aggregation and influence the crystallinity of the spray-dried samples[44]. In this study, the residual water content was determined by using Karl Fisher titration. All formulations had relatively low moisture content which followed the rank order of L-leucine (4.11 ± 0.21%, w/w) < excipient-free (4.55 ± 0.49%, w/w) < lactose (5.8 ± 0.36%, w/w) containing products. These results demonstrate that the optimized outlet air temperature

(around 65 °C) was suitable for serum albumin. The L-leucine containing formulation had the lowest water content due to the low hygroscopic behavior of this amino acid[46, 47]. The low moisture content can potentially improve the flowability and consequently enhance lung deposition due to reduced aggregation as expected. Storage conditions are also important, e.g. the spray-dried amorphous lactose particles could transform into crystals easily in humidity above 30%[48].

3.2.2. Fourier-Transform Infrared Spectroscopy (FT-IR)

FTIR analysis allows a quick and efficient identification of the compounds and by their functional groups and bond vibrations. In the spectrum of raw Api, the following characteristic regions were observed: 2710-2580 cm^{-1} O-H bond, 1730-1680 cm^{-1} C=O stretch and 1450-1380 cm^{-1} C-H bend. A broad peak observed at 3300 cm^{-1} can be attributed to O-H stretching and those bands at 1600-1400 cm^{-1} (C-C stretch in ring) and 900-675 cm^{-1} (C-H 'oop') can be assigned to the aromatic group (**Figure 4 A**). In the spectrum of BSA protein, the amide I band at 1635 cm^{-1} (mainly C=O stretch) and amide II band at 1530–1500 cm^{-1} (C–N stretching and N–H bend) can be seen. The medium broad peak at 3276 cm^{-1} corresponds to bonded N-H stretch of amide and a smaller band at 1057 cm^{-1} is the C-N stretch of aliphatic amine. In the spectra of the excipients-free formulation, the characteristic amide bands of BSA can be seen and peak at 830 cm^{-1} indicating the presence of Api (aromatic) which is an indirect confirmation of Api encapsulation on BSA-NPs. Conformational changes can be suggested due to the lack of the peak of aliphatic amine.

The spectra of raw Api, BSA, lactose and lactose containing product are displayed on **Figure 4 B**. In the spectra of lactose there is also a broad band around 3300 cm^{-1} indicating the stretching vibration of hydroxyl group. A weak band at 1654 cm^{-1} is the bending vibration of the crystalline water and peaks at 1200-1070 cm^{-1} demonstrate the stretching vibration of C-O-C in the glucose and galactose. The spectrum of amorphous lactose has the less number and

defined peaks and therefore it could be distinguished from the crystalline spectrum[49]. The characteristic broad band at 3300 cm^{-1} in the spectrum of spray-dried product could originate from the residual water content that is further supported by the Karl Fischer titration data (lactose containing product had the highest water content). Similarly to the spectrum of excipients-free formulation, the amide bands of BSA and a small peak of Api could be observed. The peaks at 1200-1070 cm^{-1} demonstrate the lactose content and the amorphous state could be assumed.

Functional groups of L-leucine lead to its characteristic spectrum (**Figure 4 C**). The strong band in the region of 2970-2910 cm^{-1} can be accounted for the aliphatic C-H stretching. The bonded N-H stretch is present in the region of 2600-2450 cm^{-1}. The NH_2 bending and the C-N skeletal vibration appear in the regions of 1595-1550 cm^{-1} and 1250-1020 cm^{-1} [50]. The presence of BSA characteristic peaks on the spray-dried formulation could be mainly observed with and a small peak of Api but the major characteristic peaks of L-leucine are obscured.

3.2.3. X-ray powder diffraction (XRPD)

XRPD is considered to be the most accurate method to study crystalline structure[51]. The combined XRPD diffractograms of Api and spray-dried formulations are presented in **Figure 5**. The characteristic narrow diffraction peaks of Api are due to the crystalline state of the commercially available material. In comparison, broad diffuse peaks could be observed in the diffractograms of the spray-dried formulations suggesting the amorphous state of BSA-Api-NPs. The observed XRD patterns of spray-dried L-leucine and lactose were consistent with literature[48, 52, 53].

3.2.4. Differential scanning calorimetry analysis (DSC)

The DSC curves of raw Api, excipents, physical mixtures and spray-dried formulations were studied to examine crystallinity. As seen in **Figure 6**, there is only one

sharp endothermic peak at 360 °C indicating the melting point of raw Api; no impurities were observed. Drug free albumin exhibited two broad peaks with onset values of 220 °C and 310 °C. The evaporation of residual water occurred at 50-120 °C. The melting point of Api on the thermograms of raw material and physical mixtures corresponds to the crystalline habitus. In the thermograms of physical mixtures on **Figure 6 B** the endothermic peak at 140 °C indicating the crystalline lactose[54] and the sublimation of L-leucine crystals occurred at 200-230 °C (**Figure 6 C**)[55]. However, in each spray-dried formulation the absence of endotherms confirms the loss of crystallinity. No peak could be observed around 360 °C indicating that Api is in amorphous state due to the spray drying process which is in agreement with the XRPD diffractograms. The amorphous form generated may result higher solubility of the powders and dissolution of apigenin in lung fluids.

3.2.5. Aerosol particle size analysis and redispersibility in water

Dry powder formulations of BSA-Api-NPs were prepared with the aim of studying the influence of excipients on the particle size and aerodynamic behavior. The deposition of aerosols is significantly affected by particle size which should be small enough to pass through the upper airways and large enough to avoid exhalation[56]. Gravitational sedimentation is the main driving force for deposition of a nanoparticulate system in the lung due to the formation of aggregates in the micrometer size range. Particle geometry and surface properties also play a significant role in reaching the bronchioles[22,32]. It is well known that particles can be deposited efficiently deeper in the lung if their aerodynamic diameter is in the range of 1-5 µm and only those with 1-3 µm can reach the respiratory zone[57]. Particles, larger than 5 µm tend to deposit in the oropharynx and the mucociliary clearance plays a role in clearing the particles towards the pharynx. However, very small particles, less than 1 µm are usually exhaled because of the low inertia[58, 59]. Mucociliary clearance is the part of the natural defense mechanism of the lung as well as the phagocytosis of macrophages in the alveolar

region. The aerosol particle size was determined by Sympatec HELOS laser diffractometer (**Table 1**). The excipient-free and lactose containing products have similar sizes while spray drying with L-leucine produced the smallest particles (D_{50}= 2.473 µm). In all cases, the particle size could ensure the highest probability of delivery of apigenin into the respiratory zone.

Following the re-dispersion of spray powders formulations in distilled water, the size of the particles was preserved in the nanometer size range: without excipient (358.9 ± 5.3 nm, PDI: 0.315 ± 0.013), lactose (366.1 ± 4.8 nm, PDI: 0.382 ± 0.014) and L-leucine (343.7 ± 2.9, PDI: 0.316 ± 0.011) containing products. The spray drying has no significant effect on the average size of the particles suggesting the deposition of apigenin containing nanoparticles in the lung fluid. Moreover, the excipients did not affect adversely the particle size.

3.2.6. Solubility and Drug release studies of BSA-Api formulations

The solubility of apigenin in nanoparticles was investigated in PBS buffer and mSLF (**Figure 7 A**). The results showed that the solubility was slightly increased in mSLF media (82-98% within 5 minutes), however, it was high in PBS buffer as well (79-95% within 5 minutes). These data indicated that the solubility of apigenin could be highly enhanced by BSA nanoparticles in aqueous medium. Nevertheless, the dispersibility enhancers could play a role in the solubility. In case of excipient free formulation, 91% of the encapsulated apigenin was dissolved in mSLF within 5 minutes. Formulation prepared with lactose increased the solubility rate up to 98%, however, it was slower (82%) when using L-leucine and completed within 2 hours. These results could be attributed to the solubility of the excipients themselves: lactose has very good water solubility, but L-leucine possess a low solubility in water[60].

The apigenin release from the spray dried BSA-Api NPs was investigated with Franz cell apparatus. It is a well known device for the dissolution of semisolid dosage forms and

approved by the USP (United States Pharmacopeia). However, there is no standardized method for inhaled powders, Franz cell could be one of the alternative choices due to simulating the diffusion controlled air-liquid interface of the lung. On the contrary, it has some limitations such as small air bubbles under the contact area of membrane to dissolution medium, wide range of standard deviation or the recovery usually around maximum 90% [61]. Based on the solubility measurements, mSLF was applied. The cumulative dissolution curves of the prepared formulations are shown in **Figure 7 B**. As expected, the dissolution was affected by the co-spray dried excipients. Lactose containing product resulted the fastest and highest apigenin release due to the excellent water solubility. This enhancement of the dissolution is supported by previously published data[62]. In contrast, the dissolution rate was decreased when L-leucine was applied. The coating layer of L-leucine slowed down the dissolution of apigenin which could be well observed in the dissolution curve. The low water solubility of L-leucine is able to hinder the dissolution of the drug which was published previously[60]. These results suggest that the excipients play an important role in the solubility and the dissolution as well.

3.2.7. Aerosol delivery of BSA-Api formulations

Particles can be taken up by alveolar macrophages which influences the therapeutic outcome. Those nanoparticles which are soluble and above 200 nm are able to escape from the macrophages therefore exhibit sustained therapeutic effect[63]. The lung deposition and therefore the efficacy of the inhaled therapeutics are governed by their aerosol properties[56]. Manufacturing respirable nanoparticles could be produced by aggregation in the favorable size range or their incorporation into microparticles (1-5 μm) [26]. Lactose monohydrate is a well-known, traditional carrier for improving the performance of inhaled products; however, it is influenced by physicochemical properties and interaction with the active ingredient[64, 65]. It is the only FDA approved carrier and has also been shown to be a potential excipient for

protein encapsulation[27, 65]. Recently, novel materials such as specific amino acids have been developed for pulmonary formulations[26] and L-leucine is one of the most effective dispersibility enhancer among them[47]. Previous studies proved that 5% (w/w) L-leucine improved the aerosol performance of raw naringin[66] and inclusion up to 15% (w/w) L-leucine resulted higher ED and FPF of powder formulation of gentamicin[46].

In this study *in vitro* aerosol properties of three different dry powders formulations were evaluated using the NGI which is regarded as an optimal instrument for analysis of aerodynamic behavior of aerosol formulations for pulmonary drug delivery[67] according to European and US Pharmacopeias. The obtained data and deposition pattern are presented in **Table 2** and in **Figure 8**. It can be seen that more than 90% of apigenin could be recovered from the NGI which is in the acceptable pharmacopeia range (75-125%). The ED ranged between 91-96% indicating good flowability and high dispersibility of the powders. L-leucine containing formulation had the highest ED as it could improve significantly the flowability of the powders [47, 53]. **Figure 8** shows the amount of Api deposited on the throat, device and stages 1-7 expressed as a percentage of the total amount of recovered powder. All formulation exhibited increased deposition in Stage 2 - 4 indicating enhanced drug delivery to the alveolar regions. As expected, improved aerosol performance and deposition (Stage 3 and 4) could be observed when L-leucine was used an as excipient. The FPF is one of the key parameters in aerosol delivery and should be as high as possible[68]. In this study, the FPF values ranged between 58-66%, suggesting that the particles could be delivered into the peripheral regions. Spray drying of nanoparticles in the presence of L-leucine resulted higher FPF value (66%) due to the improved surface properties and morphology of the particles[65]. In general, MMAD values < 5 μm are for pulmonary lung delivery and between 2-3 μm are optimal for deep lung deposition[56]. In each cases, the calculated mass median aerodynamic diameter (MMAD) data were in agreement with the physical diameter size of the particles measured by laser

diffractometer. The data obtained (< 5 μm) support good dispersibility of the particles into the lower airways and the deep lung. Therefore local delivery to the alveoli could be assured by both excipient-free and lactose formulations generated (MMAD 3.2 μm and 3.1 μm). Moreover, formulation with L-leucine (MMAD 2.1 μm) would be more optimal for deep lung deposition. The size distribution of an aerosol is described best by GSD[69]. Based on the GSD data obtained, the L-leucine containing formulation had the narrowest size distribution (1.8 μm) but that of the others was also in the acceptable range (< 3 μm).

The overall values demonstrate that the particles of each dry powder nanoparticle formulation are in the favorable aerodynamic size range, possess good dispersibility properties and particle deposition. Therefore BSA-NPs is an attractive delivery system for pulmonary drug delivery. We demonstrated that L-leucine improved better the aerosolization properties of BSA-Api-NPs than lactose monohydrate. Therefore it can be concluded that the use of excipients influence the aerosol performance of nanoparticles.

3.2.8. Particle morphology

SEM analysis was conducted to investigate the morphology of the powders (**Figure 9 A** and **B**). It is well known that the morphology of the particles is strongly affected by the solubility of the components and the nature of the excipients[46, 47]. The commercially available Api was a crystalline powder featuring needle-shaped crystals. The excipient-free spray-dried nanoparticles exhibited spherical shape and smooth or wrinkled surface. Particles of lactose containing product had raisin-like surface and some of the particles were larger in accordance with the laser diffraction particle size analysis. Powders prepared with L-leucine comprised small and collapsed particles with strongly corrugated surface. The low aqueous solubility of L-leucine leading to a shell on the surface of the droplet which interfere with the diffusion of water therefore corrugated particles could form. This outcome was consistent with previous observations[46,53,70]. Corrugated surface improves the dispersibility of the dry powder

formulations and enhance respirability due to the reduced interparticulate cohesion (Van der Waals forces) which is beneficial for particles intended for inhalation[71].

3.3. Antioxidant activity

Owing to its reproducibility and comparability, the DPPH˙ assay is an established method for investigating the antioxidant properties of natural compounds. Due to the H-donating ability of the antioxidants, a stable reduced DPPH-H molecule can form. The reaction can be seen visually and the detection can be carried out using UV-Vis spectrophotometer[72, 73]. Previous studies confirmed that Api is able to scavenge the DPPH˙ free radial even in nanoscale delivery formulation[74, 75]. In general, the scavenging activity is influenced by concentration and structural features like hydrogen donating ability, position and the degree of hydroxylation[76, 77]. In order to calculate the exact concentration of remaining DPPH˙ in the samples a calibration curve was plotted with R^2=0.9999. The time required to reach the steady state was estimated to be 120 minutes, and the slow reaction kinetic of Api has been reported[74]. The discoloration of the deep purple DPPH˙ free radical indicate the antioxidant properties of free and encapsulated Api. The inhibition of free radicals by the prepared spray-dried formulations were compared to the empty BSA-NPs, methanolic Api solution and "empty" nanoparticles (**Figure 10**). It can be seen that the free and encapsulated Api have similar scavenging activity, moreover, the spray drying did not result in the loss of scavenging activity. It has been reported that serum albumin is a physiological circulating antioxidant in the body[78] which is confirmed by the inhibition capacity of the empty BSA-NPs observed. Similar results were reported when encapsulating rutin and keampferol[79] or quercetin[17] where the antioxidant activity of the flavonoids are retained by BSA. It can be concluded that the antioxidant activity of Api is preserved, moreover, slightly enhanced by the BSA.

4. CONCLUSION

In this study novel apigenin containing albumin nanoparticles were prepared for inhalation against lung injury caused by oxidative stress. Apigenin was recently classified as a BCS II. drug with prominent antioxidant and anti-inflammatory properties in the lung. The obtained results confirmed that incorporation of apigenin into the biocompatible albumin nanoparticles resulted high encapsulation efficiency therefore it could be an attractive tool for the delivery. Moreover, the spray dried nanoparticles possess good ability to re-disperse in aqueous media and size of the particles was preserved in the nanometer size range. The influence of dispersibility enhancers on the physicochemical properties and *in vitro* pulmonary deposition were investigated and compared to the excipient-free formulation. The obtained *in vitro* pulmonary depositions proved that the developed BSA-NP dry powders are potentially able to carry apigenin deep in the lung, reaching the respiratory zone. The use of novel excipient amino acid L-leucine resulted enhanced aerodynamic properties over the traditional lactose monohydrate, indicating that the nature of the excipients and morphology of the particles play a significant role in the formulation of nanoparticles for pulmonary delivery. In addition, the solubility and dissolution characteristics of apigenin from nanoparticles were determined in mSLF dissolution media, the co-spray dried excipients played an important role. The dissolution rate was increased by the water soluble lactose and decreased by L-leucine, which has low water solubility. Therefore the use of excipients should be taken into consideration, may not required in case of albumin nanoparticles. We further confirmed that the antioxidant activity is retained, thus the potential of albumin nanoparticles as an effective pulmonary delivery system for flavonoids such as apigenin.

ACKNOWLEDGEMENTS

The authors gratefully acknowledge to Róbert Kovács for providing the SEM pictures at Budapest University of Technology and Economics.

Author Disclosure Statement

The authors declare that there are no conflicts of interest.

REFERENCES

1. Chow C-W, Herrera Abreu MT, Suzuki T, and Downey GP. Oxidative Stress and Acute Lung Injury. *Am J Respir Cell Mol Biol*. 2003;29:427-431.
2. Chen XW, Serag ES, Sneed KB, and Zhou SF. Herbal bioactivation, molecular targets and the toxicity relevance. *Chem Biol Interact*. 2011;192:161-176.
3. Patel D, Shukla S, and Gupta S. Apigenin and cancer chemoprevention: progress, potential and promise (review). *Int J Oncol*. 2007;30:233-245.
4. Kim SJ, Jeong HJ, Moon PD, Lee KM, Lee HB, Jung HJ, Jung SK, Rhee HK, Yang DC, Hong SH, and Kim HM. Anti-inflammatory activity of gumiganghwaltang through the inhibition of nuclear factor-kappa B activation in peritoneal macrophages. *Biol Pharm Bull*. 2005;28:233-237.
5. Kowalski J, Samojedny A, Paul M, Pietsz G, and Wilczok T. Effect of apigenin, kaempferol and resveratrol on the expression of interleukin-1beta and tumor necrosis factor-alpha genes in J774.2 macrophages. *Pharmacol Rep*. 2005;57:390-394.
6. Lee J-H, Zhou H, Cho S, Kim Y, Lee Y, and Jeong C. Anti-inflammatory mechanisms of apigenin: inhibition of cyclooxygenase-2 expression, adhesion of monocytes to human umbilical vein endothelial cells, and expression of cellular adhesion molecules. *Archives of Pharmacal Research*. 2007;30:1318-1327.
7. Chen L and Zhao WEI. Apigenin protects against bleomycin-induced lung fibrosis in rats. *Exp Ther Med*. 2016;11:230-234.
8. Luan RL, Meng XX, and Jiang W. Protective Effects of Apigenin Against Paraquat-Induced Acute Lung Injury in Mice. *Inflammation*. 2016; 39:752-758.
9. Basios N, Lampropoulos P, Papalois A, Lambropoulou M, Pitiakoudis MK, Kotini A, Simopoulos C, and Tsaroucha AK. Apigenin Attenuates Inflammation in

Experimentally Induced Acute Pancreatitis-Associated Lung Injury. *J Invest Surg*. 2015;2:1-7.

10. Patil R, Babu RL, Naveen Kumar M, Kiran Kumar KM, Hegde S, Ramesh G, and Chidananda Sharma S. Apigenin inhibits PMA-induced expression of pro-inflammatory cytokines and AP-1 factors in A549 cells. *Mol Cell Biochem*. 2015;403:95-106.

11. Wang J, Liu Y-T, Xiao L, Zhu L, Wang Q, and Yan T. Anti-Inflammatory Effects of Apigenin in Lipopolysaccharide-Induced Inflammatory in Acute Lung Injury by Suppressing COX-2 and NF-kB Pathway. *Inflammation*. 2014;37:2085-2090.

12. Zhang J, Liu D, Huang Y, Gao Y, and Qian S. Biopharmaceutics classification and intestinal absorption study of apigenin. *Int J Pharm*. 2012;436:311-317.

13. Ajazuddin and Saraf S. Applications of novel drug delivery system for herbal formulations. *Fitoterapia*. 2010;81:680-689.

14. Elzoghby AO, Samy WM, and Elgindy NA. Albumin-based nanoparticles as potential controlled release drug delivery systems. *J Control Release*. 2012;157:168-182.

15. Hu Y-J, Liu Y, Sun T-Q, Bai A-M, Lü J-Q, and Pi Z-B. Binding of anti-inflammatory drug cromolyn sodium to bovine serum albumin. *Int J Biol Macromolec*. 2006;39:280-285.

16. Fasano M, Curry S, Terreno E, Galliano M, Fanali G, Narciso P, Notari S, and Ascenzi P. The extraordinary ligand binding properties of human serum albumin. *IUBMB Life*. 2005;57:787-796.

17. Fang R, Hao R, Wu X, Li Q, Leng X, and Jing H. Bovine Serum Albumin Nanoparticle Promotes the Stability of Quercetin in Simulated Intestinal Fluid. *J Agr Food Chem*. 2011;59:6292-6298.

18. He X, Xiang N, Zhang J, Zhou J, Fu Y, Gong T, and Zhang Z. Encapsulation of teniposide into albumin nanoparticles with greatly lowered toxicity and enhanced antitumor activity. *Int J Pharm*. 2015;487:250-259.

19. Muralidharan P, Malapit M, Mallory E, Hayes Jr D, and Mansour HM. Inhalable nanoparticulate powders for respiratory delivery. *Nanomedicine: NBM*. 2015;11:1189-1199.

20. Malcolmson RJ and Embleton JK. Dry powder formulations for pulmonary delivery. *Pharm Sci Technol To*. 1998;1:394-398.

21. Stegemann S, Kopp S, Borchard G, Shah VP, Senel S, Dubey R, Urbanetz N, Cittero M, Schoubben A, Hippchen C, Cade D, Fuglsang A, Morais J, Borgström L, Farshi F, Seyfang KH, Hermann R, van de Putte A, Klebovich I, and Hincal A. Developing and advancing dry powder inhalation towards enhanced therapeutics. *Eur J Pharm Sci.* 2013;48:181-194.

22. Yang W, Peters JI, and Williams Iii RO. Inhaled nanoparticles—A current review. *Int J Pharm*. 2008;356:239-247.

23. Geiser M. Update on macrophage clearance of inhaled micro- and nanoparticles. *J Aerosol Med Pulm Drug Deliv*. 2010;23:207-217.

24. Woods A, Patel A, Spina D, Riffo-Vasquez Y, Babin-Morgan A, de Rosales RT, Sunassee K, Clark S, Collins H, Bruce K, Dailey LA, and Forbes B. In vivo biocompatibility, clearance, and biodistribution of albumin vehicles for pulmonary drug delivery. *J Control Release*. 2015;210:1-9.

25. Swarbrick J. *Encyclopedia of Pharmaceutical Technology*. Informa Healthcare:London; 2007; 671 - 1434.

26. Mansour HM, Rhee YS, and Wu X. Nanomedicine in pulmonary delivery. *Int J Nanomedicine*. 2009;4:299-319.

27. Shoyele SA and Cawthorne S. Particle engineering techniques for inhaled biopharmaceuticals. *Adv Drug Deliv Rev*. 2006;58:1009-1029.

28. Sung JC, Pulliam BL, and Edwards DA. Nanoparticles for drug delivery to the lungs. *Trends Biotechnol*. 2007;25:563-570.

29. Desai NP, Tao C, Yang A, Louie L, Yao Z, Soon-Shiong P, and Magdassi S. Protein stabilized pharmacologically active agents, methods for the preparation thereof and methods for the use thereof. Google Patents, 2004. US6749868 B1

30. Son YJ, McConville JT. Development of a standardized dissolution test method for inhaled pharmaceutical formulations. *Int J Pharm*. 2009;382:15–22.

31. Hatano T. KH, Yasuhara T., Okuda T. 2 new flavonoids and other constituents in licorice root-their relative astringency and radical scavenging effects. *Chem Pharm Bull*. 1988;36:2090-2097.

32. Paranjpe M and Muller-Goymann CC. Nanoparticle-mediated pulmonary drug delivery: a review. *Int J Mol Sci*. 2014;15:5852-5873.

33. Kim TH, Jiang HH, Youn YS, Park CW, Tak KK, Lee S, Kim H, Jon S, Chen X, and Lee KC. Preparation and characterization of water-soluble albumin-bound curcumin nanoparticles with improved antitumor activity. *Int J Pharm*. 2011;403:285-291.

34. Wei Y, Li L, Xi Y, Qian S, Gao Y, and Zhang J. Sustained release and enhanced bioavailability of injectable scutellarin-loaded bovine serum albumin nanoparticles. *Int J Pharm*. 2014;476:142-148.

35. Valeur B. *Molecular fluorescence principles and applications*. Wiley-VCH: Weinheim; 2002; 73-124.

36. Yuan J-L, lv Z, Liu Z-G, Hu Z, and Zou G-L. Study on interaction between apigenin and human serum albumin by spectroscopy and molecular modeling. *J Photochem Photobiol A*. 2007;191:104-113.

37. Naveenraj S and Anandan S. Binding of serum albumins with bioactive substances – Nanoparticles to drugs. *J Photochem Photobiol C*. 2013;14:53-71.

38. Tayeh N, Rungassamy T, and Albani JR. Fluorescence spectral resolution of tryptophan residues in bovine and human serum albumins. *J Pharm Biomed Anal*. 2009;50:107-116.

39. Zhao X-N, Liu Y, Niu L-Y, and Zhao C-P. Spectroscopic studies on the interaction of bovine serum albumin with surfactants and apigenin. *Spectrochim Acta A Mol Biomol Spectrosc*. 2012;94:357-364.

40. Lin C-Z, Hu M, Wu A-Z, and Zhu C-C. Investigation on the differences of four flavonoids with similar structure binding to human serum albumin. *J Pharm Anal*. 2014;4:392-398.

41. Cao H, Liu Q, Shi J, Xiao J, and Xu M. Comparing the Affinities of Flavonoid Isomers with Protein by Fluorescence Spectroscopy. *Anal Lett*. 2008;41:521-532.

42. Shang Y and Li H. Studies of the interaction between apigenin and bovine serum albumin by spectroscopic methods. *Russ J Gen Chem*. 2010;80:1710-1717.

43. Tang L, Jia W, and Zhang D. The effects of experimental conditions of fluorescence quenching on the binding parameters of apigenin to bovine serum albumin by response surface methods. *Luminescence*. 2014;29:344-351.

44. Stahl K, Claesson M, Lilliehorn P, Linden H, and Backstrom K. The effect of process variables on the degradation and physical properties of spray dried insulin intended for inhalation. *Int J Pharm*. 2002;233:227-237.

45. Jensen DM, Cun D, Maltesen MJ, Frokjaer S, Nielsen HM, and Foged C. Spray drying of siRNA-containing PLGA nanoparticles intended for inhalation. *J Control Release*. 2010;142:138-145.

46. Aquino RP, Prota L, Auriemma G, Santoro A, Mencherini T, Colombo G, and Russo P. Dry powder inhalers of gentamicin and leucine: formulation parameters, aerosol performance and in vitro toxicity on CuFi1 cells. *Int J Pharm*. 2012;426:100-107.

47. Yang X-F, Xu Y, Qu D-S, and Li H-Y. The influence of amino acids on aztreonam spray-dried powders for inhalation. *Asian J Pharm Sci*. 2015;10:541-548.

48. Wu L, Miao X, Shan Z, Huang Y, Li L, Pan X, Yao Q, Li G, and Wu C. Studies on the spray dried lactose as carrier for dry powder inhalation. *Asian J Pharm Sci*. 2014;9:336-341.

49. Listiohadi Y, Hourigan J, Sleigh R, and Steele R. Thermal analysis of amorphous lactose and α-lactose monohydrate. *Dairy Sci Technol*. 2009;89:43-67.

50. Němec I and Mička Z. FTIR and FT Raman study of L-leucine addition compound with nitric acid. *J Mol Struct*. 1999;482–483:23-28.

51. Newman AW and Byrn SR. Solid-state analysis of the active pharmaceutical ingredient in drug products. *Drug Discov Today*. 2003;8:898-905.

52. Sou T, Kaminskas LM, Nguyen T-H, Carlberg R, McIntosh MP, and Morton DAV. The effect of amino acid excipients on morphology and solid-state properties of multi-component spray-dried formulations for pulmonary delivery of biomacromolecules. *Eur J Pharm Biopharm*. 2013;83:234-243.

53. Mangal S, Meiser F, Tan G, Gengenbach T, Denman J, Rowles MR, Larson I, and Morton DAV. Relationship between surface concentration of l-leucine and bulk powder properties in spray dried formulations. *Eur J Pharm Biopharm*. 2015;94:160-169.

54. Gombás Á, Szabó-Révész P, Kata M, Regdon G, Jr., and Erős I. Quantitative Determination of Crystallinity of α-Lactose Monohydrate by DSC. *J Therm Anal Calorim.* 2002;68:503-510.

55. Raula J, Seppälä J, Malm J, Karppinen M, and Kauppinen EI. Structure and Dissolution of l-Leucine-Coated Salbutamol Sulphate Aerosol Particles. *AAPS PharmSciTech*. 2012;13:707-712.

56. Yang MY, Chan JGY, and Chan H-K. Pulmonary drug delivery by powder aerosols. *J Control Release*. 2014;193:228-240.

57. Chow AL, Tong HY, Chattopadhyay P, and Shekunov B. Particle Engineering for Pulmonary Drug Delivery. *Pharm Res*. 2007;24:411-437.

58. Liang Z, Ni R, Zhou J, and Mao S. Recent advances in controlled pulmonary drug delivery. *Drug Discov To*. 2015;20:380-389.

59. Heyder J, Gebhart J, Rudolf G, Schiller CF, and Stahlhofen W. Deposition of particles in the human respiratory tract in the size range 0.005–15 μm. *J Aerosol Sci*. 1986;17:811-825.

60. Raula J, Seppälä J, Malm J, Karppinen M, Kauppinen EI. Structure and dissolution of L-leucine-coated salbutamol sulphate aerosol particles. *AAPS PharmSciTech*. 2012; 13:707-12.

61. May S, Jensen B, Wolkenhauer M, Schneider M, Lehr CM. Dissolution techniques for in vitro testing of dry powders for inhalation. *Pharm Res*. 2012;29:2157-66.

62. Knieke C, Azad MA, To D, Bilgili E, Davé RN. Sub-100 micron fast dissolving nanocomposite drug powders. *Powder Technol*. 2015;271:49–60.

63. Patel B, Gupta N, and Ahsan F. Particle engineering to enhance or lessen particle uptake by alveolar macrophages and to influence the therapeutic outcome. *Eur J Pharm Biopharm*. 2015;89:163-174.

64. Kou X, Chan LW, Steckel H, and Heng PWS. Physico-chemical aspects of lactose for inhalation. *Adv Drug Deliv Rev*. 2012;64:220-232.

65. Pilcer G, Wauthoz N, and Amighi K. Lactose characteristics and the generation of the aerosol. *Adv Drug Deliv Rev*. 2012;64:233-256.

66. Prota L, Santoro A, Bifulco M, Aquino RP, Mencherini T, and Russo P. Leucine enhances aerosol performance of Naringin dry powder and its activity on cystic fibrosis airway epithelial cells. *Int J Pharm*. 2011;412:8-19.

67. Taki M, Marriott C, Zeng X-M, and Martin GP. Aerodynamic deposition of combination dry powder inhaler formulations in vitro: A comparison of three impactors. *Int J Pharm*. 2010;388:40-51.

68. Davis SS. Delivery of peptide and non-peptide drugs through the respiratory tract. *Pharm Sci Techn To*. 1999;2:450-456.

69. Musante CJ, Schroeter JD, Rosati JA, Crowder TM, Hickey AJ, and Martonen TB. Factors affecting the deposition of inhaled porous drug particles. *J Pharm Sci*. 2002;91:1590-1600.

70. Lechuga-Ballesteros D, Charan C, Stults CL, Stevenson CL, Miller DP, Vehring R, Tep V, and Kuo MC. Trileucine improves aerosol performance and stability of spray-dried powders for inhalation. *J Pharm Sci*. 2008;97:287-302.

71. Chew NY and Chan HK. The role of particle properties in pharmaceutical powder inhalation formulations. *J Aerosol Med*. 2002;15:325-330.

72. Brand-Williams W, Cuvelier ME, and Berset C. Use of a free radical method to evaluate antioxidant activity. *LWT - Food Science and Technology*. 1995;28:25-30.

73. Villaño D, Fernández-Pachón MS, Moyá ML, Troncoso AM, and García-Parrilla MC. Radical scavenging ability of polyphenolic compounds towards DPPH˙ free radical. *Talanta*. 2007;71:230-235.

74. Al Shaal L, Shegokar R, and Muller RH. Production and characterization of antioxidant apigenin nanocrystals as a novel UV skin protective formulation. *Int J Pharm*. 2011;420:133-140.

75. Papay Z.E AI. Study on the antioxidant activity during the formulation of biological active ingredient. *European Scientific Journal*. 2014;Special Edition 3:252-257.

76. Yang J, Guo J, and Yuan J. In vitro antioxidant properties of rutin. *LWT - Food Science and Technology*. 2008;41:1060-1066.

77. Natella F, Nardini M, Di Felice M, and Scaccini C. Benzoic and Cinnamic Acid Derivatives as Antioxidants: Structure−Activity Relation. *J Agr Food Chem*. 1999;47:1453-1459.

78. Roche M, Rondeau P, Singh NR, Tarnus E, and Bourdon E. The antioxidant properties of serum albumin. *FEBS Lett*. 2008;582:1783-1787.

79. Fang R, Jing H, Chai Z, Zhao G, Stoll S, Ren F, Liu F, and Leng X. Study of the physicochemical properties of the BSA: flavonoid nanoparticle. *Eur Food Res Technol*. 2011;233:275-283.

TABLES

Table 1

Aerosol particle sizes of spray-dried nanoparticles with Sympatec HELOS laser diffractometer in µm.

	Excipient-free	Lactose	L-leucine
ED (%)	91.862 ± 2.735	93.950 ± 1.046	95.183 ± 0.667
FPF (%)	65.617 ± 3.422	58.463 ± 6.031	66.090 ± 2.777
MMAD (µm)	3.210 ± 0.069	3.130 ± 0.001	2.123 ± 0.098
GSD (µm)	2.823 ± 0.113	2.270 ± 0.212	1.887 ± 0.063
RD (%)	99.1 ± 5.012	94.7 ± 4.091	96.3 ± 2.161

Table 2

Aerodynamic characteristic of spray-dried nanoparticles.

	Excipient-free	Lactose	L-leucine
D_{10}	1.033 ± 0.032	1.020 ± 0.070	0.843 ± 0.680
D_{50}	3.030 ± 0.092	3.107 ± 0.102	2.473 ± 0.300
D_{90}	7.110 ± 0.306	7.117 ± 0.337	5.287 ± 0.670

FIGURE CAPTIONS

Figure 1. Molecular structure of apigenin.

Figure 2. Fluorescence emission spectra of BSA solution, BSA nanoparticles and BSA-Api nanoparticles. The excitation wavelength was set to 285 nm (EM: emission, EXC: excitation)

Figure 3. Three dimensional fluorescence emission maps and two dimensional contour maps of empty BSA nanoparticles and BSA-Api nanoparticles. Color scale displays the range of observed fluorescence intensities.

Figure 4. **A)** FT-IR spectra of apigenin (1), BSA (2) and the excipient-free spray-dried BSA-Api nanoparticles (3).

B) FT-IR spectra of apigenin (1), BSA (2), lactose (3) and the spray-dried BSA-Api nanoparticles with lactose (4).

C) FT-IR spectra of apigenin (1), BSA (2), L-leucine (3) and the spray-dried BSA-Api nanoparticles with L-leucine (4).

Figure 5. XRPD diffraction pattern of raw apigenin and the formulations.

Figure 6. **A)** DSC thermograms of apigenin (1), BSA (2) physical mixture (3) and the excipient-free spray dried BSA-Api nanoparticles (4).

B) DSC spectra of apigenin (1), BSA (2), physical mixture (3) and the spray-dried BSA-Api nanoparticles with lactose (4).

C) DSC spectra of apigenin (1), BSA (2), physical mixture (3) and the spray-dried BSA-Api nanoparticles with L-leucine (4).

Figure 7. **A)** Solubility of spray dried BSA-Api formulations in PBS buffer and modified simulated lung fluid (mSLF).

B) Dissolution of apigenin from the formulations as a function of time in modified simulated lung fluid (mSLF).

Figure 8. NGI deposition pattern of the spray dried BSA-Api formulations.

Figure 9. SEM images of raw apigenin (1), excipient-free spray dried BSA-Api nanoparticles (2), spray-dried BSA-Api nanoparticles with lactose (3), spray-dried BSA-Api nanoparticles with L-leucine (4) 20000 x magnification.

Figure 10. Radical scavenging activity of Apigenin solution, empty BSA nanoparticles, BSA-Apigenin nanoparticles (NP) and spray-dried nanoparticles (SD) with excipients. The antioxidant activity is expressed as the inhibition of DPPH˙ free radical in percent.

To whom correspondence should be addressed:

antal.istvan@pharma.semmelweis-univ.hu

Department of Pharmaceutics

Semmelweis University

Hőgyes E. Street 7-9,

H-1092 Budapest, Hungary

Tel/Fax: +3612017-0914; Tel.: +361476-3600/53066, 53087

Study on the pulmonary delivery system of apigenin loaded albumin nanocarriers with antioxidant activity

Zsófia Edit Pápay[1], Annamária Kósa, PhD[2], Béla Böddi, PhD [2], Zahra Merchant[3], Imran Y Saleem, PhD [4], Mohammed Gulrez Zariwala, PhD[5], Imre Klebovich, PhD [1], Satyanarayana Somavarapu, PhD [3*], István Antal, PhD [1*]

[1] Department of Pharmaceutics, Semmelweis University, Hőgyes E. Street 7-9, H-1092 Budapest, Hungary

[2] Department of Plant Anatomy, Institute of Biology, Eötvös Lóránd University, Pázmány Péter Street 1/C, Budapest, Hungary

[3] Department of Pharmaceutics, UCL School of Pharmacy, 29-39 Brunswick Square, London WC1N 1AX, United Kingdom

[4] Formulation and Drug Delivery Research, School of Pharmacy and Biomolecular Sciences, Liverpool John Moores University, Liverpool, United Kingdom

[5] Department of Biomedical Science, Faculty of Science and Technology, University of Westminster, 115 New Cavendish Street, London, W1W 6UW, United Kingdom

* To whom correspondence should be addressed:

antal.istvan@pharma.semmelweis-univ.hu

Department of Pharmaceutics

Semmelweis University

Hőgyes E. Street 7-9,

H-1092 Budapest, Hungary

Tel/Fax: +3612017-0914; Tel.: +361476-3600/53066, 53087

Running title:

Albumin-Apigenin Nanoparticles against Lung Injury

ABSTRACT

Background: Respiratory diseases are mainly derived from acute and chronic inflammation of the alveoli and bronchi. The pathophysiological mechanisms of pulmonary inflammation mainly arise from oxidative damage that could ultimately lead to acute lung injury (ALI). Apigenin (Api) is a natural polyphenol with prominent antioxidant and anti-inflammatory properties in the lung. Inhalable formulations consist of nanoparticles (NPs) have several advantages over other administration routes therefore this study investigated the application of apigenin loaded bovine serum albumin nanoparticles (BSA-Api-NPs) for pulmonary delivery.

Methods: Dry powder formulations of BSA-Api-NPs were prepared by spray drying and characterized by laser diffraction particle sizing, scanning electron microscopy, differential scanning calorimetry and powder X-ray diffraction. The influence of dispersibility enhancers (lactose monohydrate and L-leucine) on the *in vitro* aerosol deposition using a next generation impactor (NGI) was investigated in comparison to excipient-free formulation. The dissolution of Api was determined in simulated lung fluid by using Franz cell apparatus. The antioxidant activity was determined by 2,2-Diphenyl-1-picrylhydrazyl (DPPH$^{\bullet}$) free radical scavenging assay.

Results: The encapsulation efficiency and the drug loading was measured to be 82.61 ± 4.56% and 7.51 ± 0.415%. The optimized spray drying conditions were suitable to produce particles with low residual moisture content. The spray dried BSA-Api-NPs possessed good the aerodynamic properties due to small and wrinkled particles with low mass median aerodynamic diameter, high emitted dose and fine particle fraction. The aerodynamic properties was enhanced by leucine and decreased by lactose, however, the dissolution was reversely affected. The DPPH$^{\bullet}$ assay confirmed that the antioxidant activity of encapsulated Api was preserved.

Conclusion: This study provides evidence to support that albumin nanoparticles are suitable carriers of Api and the use of traditional or novel excipients should be taken into consideration. The developed BSA-Api-NPs is a novel delivery system against lung injury with potential antioxidant activity.

Keywords: aerosol distribution, inhaled therapy, modeling

1. INTRODUCTION

Respiratory diseases are thought to be mainly derived from acute and chronic inflammation of the alveoli and the bronchi. The pathophysiological mechanisms of pulmonary inflammation arise from several factors, including oxidative damage due to cytotoxic mediators that may ultimately lead to acute lung injury (ALI), acute respiratory distress syndrome (ARDS) and cancer[1]. A growing body of scientific data suggests that natural occurring compounds possess preventive and therapeutic properties with inherent low toxicity[2]. Among phytochemicals, apigenin (Api, **Figure 1**) is a promising candidate as a therapeutic agent, mainly due to its antioxidant and anti-inflammatory properties[3-6]. It has been demonstrated that Api has protective effects against bleomycin-induced lung fibrosis in rats which is associated with its antioxidant and anti-inflammatory capacities[7]. Another study provided evidence that Api has was able to decrease oxidative stress and inflammation on paraquat-induced ALI in mice[8] and reduced the pathological alterations of pulmonary tissue in acute pancreatitis associated ALI, therefore suggesting protection in the lung[9]. Furthermore, Api has anti-inflammatory effect owing to significant inhibition of pro-inflammatory cytokines, activator protein (AP-1) and cyclooxygenase-2 (COX-2) in human pulmonary epithelial cells[10] and in mice as well[11]. However, Api's has low water solubility (2.16 μg/ml at pH 7.5) and therefore it was recently classified as BCS (Biopharmaceutical Classification System) II. drug[12].

Encapsulation and delivery of phytoconstituents with health effects has attracted much attention in recent years. Developing a suitable carrier system is essential to improve the overall activity and reduce the possible toxicity of these agents[13]. Among the potential carrier systems, serum albumin nanoparticles have notable advantages including biodegradability, non-antigenicity and cell-targeting ability[14,15]. Moreover, albumin provide exceptional ligand binding capacity for various drugs owing to three homologous domains with two separate

helical subdomains[16]. Studies reported the successful incorporation of flavonoids into albumin nanoparticles that can improve their stability[17] and antitumor activity[18].

Pulmonary delivery of pharmacologically active ingredients are extensively studied due to prominent advantages over other delivery routes of administration[19]. The lungs have a large surface area, limited enzymatic activity and high permeability therefore drugs can be delivered either locally for the treatment of respiratory diseases or systematically in order to e.g. avoid first pass metabolism[20]. Dry Powder Inhaler (DPI) products offer precise and reproducible delivery of fine drug particle fraction to the deep lung and recent studies have proved that these are more cost effective than other products[21]. This non-invasive delivery route could be suitable for poorly water soluble drugs in nanoparticles with increased solubility[22]. It is also well recognized that nanoparticles have benefits over other carriers in the micron scale such as controlled drug release, avoiding mucociliary clearance and improve deposition[23, 24]. Albumin is naturally present in the body, as well as in the lung epithelium[24], moreover, the body can absorb proteins into the bloodstream by transcytosis which occurs deep in the lung and allows drug molecules to pass through cell membrane[25]. Therefore the presence of BSA in the nanoparticle system increases membrane permeability, may facilitate epithelial cell uptake and translocation through the alveo-capillary barrier of the lung[26]. It was proved that albumin nanoparticles have high biocompatibility in a wide dose range and remained longer in the lungs with low systemic exposure[24]. Thus encapsulation of apigenin into albumin nanoparticles would enhance its solubility and distribution in the lung. However, the formulation of dry powders with optimal aerodynamic properties for pulmonary drug delivery is challenging. Spray drying is a technique for manufacturing respirable dry powders in one step. During the process, the liquid phase is atomized into droplets that dry rapidly in the drying chamber due to the compressed air. The process conditions like heat, flow rate, aspiration rate and pump rate also determine the quality of the product. The thermal

degradation caused by overheating can be avoided by the rapid evaporation of the solvent[27]. Hence, it is suitable for drying colloidal systems resulting in uniform particle morphology. Nanoparticle delivery systems targeted to the lungs offer several advantages such as sustained release, increased local drug concentration and targeted site of action[28]. Moreover, improved drug solubility, uniform dose distribution and fewer side effects can be achieved, compared to conventional dry powders. In general, respirable nanoparticles are embedded in microparticles in aerodynamic size range [26].

The aim of this work was to develop a novel dry powder formulation against ALI caused by oxidative stress. The prepared albumin nanoparticles were characterized in terms of size, zeta potential and drug loading, additionally the fluorescence properties were investigated. Following this, the nanoparticles were spray dried with two types of excipients, namely a traditional lactose monohydrate and a novel amino acid, L-leucine. *In vitro* aerosol deposition patterns were determined in comparison to excipient-free formulation using a next generation impactor (NGI) and dissolution test was performed in simulated lung fluid by using Franz cell apparatus. Laser diffraction particle sizing, morphology and residual moisture content were measured along with the antioxidant activity.

2. MATERIALS AND METHODS

MATERIALS

Apigenin (Api) was purchased from (purity > 99%) Hangzhou Dadyangchem Co., Ltd. (China). Bovine serum albumin powder (BSA, purity ≥ 98%), L-leucine, analytical grade chloroform, acetonitrile and trifluoroacetic acid (TFA) were obtained from Sigma Aldrich Ltd. (Dorset, UK). Lactohale® LH 230 was supplied by Friesland Foods Domo (Amersfoort, The Netherlands). 2,2-Diphenyl-1-picrylhydrazyl (DPPH˙) free radical was purchased from Sigma-Aldrich (Darmstadt, Germany). For the solubility and drug release study, PBS buffer was purchased (Sigma Aldrich Ltd., Dorset, UK) and simulated lung fluid modified with

0.02% (w/v) (mSLF) was prepared. All of the materials for the mSLF were purchased from Sigma Aldrich Ltd. (Dorset, UK).

METHODS

2.1. Preparation of BSA-NPs

BSA nanoparticles were prepared using a nanoparticle albumin bound technology with minor modifications[29]. Briefly, 1000 mg of BSA was dissolved in 50 ml of distilled water saturated with chloroform. Separately, 100 mg of Api was dissolved in 3 ml of chloroform saturated with water and ultrasonicated for 10 minutes. These two solutions were mixed and ultrasonicated for 20 minutes with a probe-type sonicator (MSE Soniprep 150 Ultrasonic Processor, MSE Ltd., London, UK) on ice. After homogenization, the chloroform was evaporated by rotary evaporator (Rotavapor® R-10, BÜCHI Labortechnik AG, Flawil, Switzerland) at 25°C for 15 minutes. The obtained nanoparticles were filtered through filter paper (0.45µm, Ficher Scientific Ltd., Loughborough, UK) and further spray dried.

2.2. Characterization of BSA-Api-NPs

2.2.1. Particle size and zeta potential analysis

The average particle size and polydispersity index (PDI) were determined by dynamic light scattering (DLS) using Zetasizer Nano ZS instrument (Malvern Instruments Ltd., Worcestershire, UK). Zeta potential of the particles was quantified with laser doppler velocimetry (LDV) using the same instrument. All measurements were performed in triplicate (n=3) at 25 °C and presented as mean ± standard deviation (SD).

2.2.2. Determination of drug loading and encapsulation efficiency

To determine the amount of Api, 1 ml sample from the BSA-Api formulation was withdrawn and the apigenin content was determined in mg/ml by adding 5 ml of dimethyl sulfoxide and methanol (DMSO:MeOH, 50:50% v/v) and sonicated for 10 minutes. The exact concentrations were determined after filtration (0.22 µm) by HPLC 1260 (Agilent

Technologies Inc., Santa Clara, USA) using reverse-phase C_{18} column (Phenomenex®, 250x4.6 mm, 4µm) as the stationary phase. The temperature was set to 25 °C. The mobile phase consisted of 40% acetonitrile and 60% water containing 0.1% (v/v) TFA. The system was run isocratically at the flow rate of 1.2 ml/min and the Api was detected at 340 nm (t_R = 8.3). The injection volume was set to 10 µl. A calibration curve was conducted by diluting stock solution (0.1 mg/ml) with R^2 value of 0.999.

The drug loading efficiency (DL, %) and encapsulation efficiency (EE, %) were calculated according to the equations (Eq. 1. and 2.), comparing the encapsulated Api content (mg/ml, $W_{encapsulated}$) to total nanoparticle system which means the weighted amount of BSA and Api together (mg/ml, W_{total}) and the amount of Api (mg/ml, $W_{theoretical}$) used in the formulations.

$$DL\ (\%) = \frac{W_{encapsulated}}{W_{total}} \times 100 \qquad \text{Eq.1.}$$

$$EE\ (\%) = \frac{W_{encapsulated}}{W_{theoretical}} \times 100 \qquad \text{Eq.2.}$$

2.2.3. Fluorescence spectroscopy

The fluorescence emission spectra of BSA and BSA-Api-NPs were measured with Jobin Yvon-Horiba Fluoromax-3 (Paris, France) spectrofluorometer. The samples which contained the nanoparticles were diluted 10 times and the fluorescence emission spectra were recorded between 300 and 450 nm at 25 °C where the excitation wavelength was set to 285 nm. The data collection frequency was 0.5 nm and the integration time was 0.2 s. The excitation slit was set at a bandpass width of 2 nm and the emission slit at 5 nm. Each spectrum was recorded three times and the mean values were calculated automatically. The SPSERV V3.14 software (© Csaba Bagyinka, Institute of Biophysics, Biological Research Center of the Hungarian Academy of Sciences, Szeged, Hungary) was used for baseline correction, for five point linear smoothing and for the correction to the wavelength-dependent

sensitivity changes of the spectrofluorometer. The subtraction of the Raman band at 390 nm was performed.

To obtain the three-dimensional projections and contour maps of fluorescence spectra of the samples, the fluorescence emission were recorded from 265 to 450 nm using different excitation wavelengths from 250 to 310 nm with 10 nm-steps with the same instrument mentioned above. All emission scan ranges were set to start at least 15 nm away from the corresponding excitation wavelengths. Other settings were similar as described above. Each spectrum was recorded three times and the mean values were calculated automatically. The three-dimensional fluorescence spectra were visualized with the software SURFER Version 10 (Golden Software, Inc., Colorado, USA). Spectra were combined together into a three dimensional surface data set with axes of excitation and emission wavelengths and fluorescence intensity. Data were also converted into two dimensional contour maps.

2.3. Spray drying of BSA-Api-NPs

Spray drying of the BSA-Api formulations without excipient and in the presence of lactose monohydrate (50%, w/w) and L-leucine (9%, w/w) were carried out in a Büchi 290 Mini Spray Dryer (BÜCHI Labortechnik AG, Flawil, Switzerland). The concentration of the excipients were with respect to the mass of the nanoparticles before spray drying. The following operating conditions were used based on pilot experiments: inlet temperature 120 °C, approximate outlet temperature 65-70 °C, the drying airflow 600 L/h, aspiration rate 100% (35 m^3/h), the nozzle diameter was a 0.1 mm and the liquid feed rate was set to 5 ml/min. Each preparation were carried out in triplicate. Following spray drying, the powders were collected from the lower part of the cyclone and the collecting vessel, stored in tightly sealed glass vials under vacuum at room temperature.

2.4. Characterization of spray-dried BSA-Api-NPs

2.4.1. Determination of residual moisture

The moisture content of the spray-dried powders was measured by using Karl Fischer titration (Metrohm 758 KFD Titirino, Metrohm AG, Lichtenstein, Switzerland). For that purpose approx. 100 mg of the product was analysed and the instrument was previously calibrated with 10 µl distilled water. The evaluation was conducted in triplicate and the standard deviation calculated.

2.4.2. Fourier-Transform Infrared Spectroscopy (FT-IR)

FT-IR spectra of BSA-Api spray-dried samples were evaluated using a PerkinElmer Spectrum 100 FT-IR spectrometer equipped with Universal ATR (Attenuated Total Reflectance) accessory (PerkinElmer Inc., Waltham, USA). Approximately 2 mg of the solid samples were placed between the plate and the probe. The spectra were recorded with 3 scans, in the frequency range between 4000-600 cm^{-1} and with a resolution of 4 cm^{-1} at room temperature. The data were analyzed using the PerkinElmer Spectrum Express software.

2.4.3. X-ray powder diffraction (XRPD)

XRPD diffractograms were obtained using an X-ray diffractometer (MiniFlex600 Rigaku Corporation, Tokyo, Japan). The analyses were performed at room temperature and the samples were scanned from 2° to 40° 2θ using a scanning speed of 2°/min with a step size of 0.05°.

2.4.4. Differential scanning calorimetry (DSC) analysis

The spray-dried formulations were characterized by DSC (DSC Q2000 module; TA Instruments, New Castle, UK) which was calibrated using indium. Samples (3-5 mg) were weighed accurately and analyzed in sealed and pierced aluminium hermetic pans (TA Instruments). The pans were equilibrated at 25 °C and then heated at a rate of 10 °C/min in a range of 50–400 °C.

2.4.5. Aerosol particle size analysis and redispersibility in water

The particle size analysis was conducted by using a Sympatec HELOS laser diffractometer (Sympatec GmbH System-Partikel-Technik, Clausthal-Zellerfeld, Germany). The powders were dispersed by compressed air (4-5 bar) into the measuring zone of the laser beam. The optical lens (0.45–87.5 µm size range) focused onto the detector to collect the diffracted light for calculation of size distribution. The values of 10th (D_{10}), 50th (D_{50}) and 90th (D_{90}) of the cumulative particle size distribution are generated. Samples were measured in triplicate.

The particle size was also determined after spray drying. 5 mg dry powder of each formulation could be easily redispersed in 5 ml distilled water and the particle size was determined without any further dilution by the above mentioned Zetasizer Nano ZS instrument (Malvern Instruments Ltd., Worcestershire, UK).

2.4.6. Solubility and Drug release studies of BSA-Api formulations

The solubility of BSA-Api formulations were determined in PBS buffer (pH 7.4) and in modified simulated lung fluid (mSLF, pH 7.4) which contained 0.02% (w/v) DPPC was prepared according to Son and McConville[30]. 50 mg of samples of spray dried powders were added to 100 mL solvent and shaken (150 rpm) for 2 h at 37 °C. At predetermined time points 1 mL of samples were taken from each dissolution media and replaced with the same volume of fresh medium. All of the samples were diluted with 1 ml methanol and filtered with Amicon® Ultra Centrifugal filters (30K, Merck Millipore, Merck KGaA, Germany) prior to the injection and the amount of apigenin was determined by HPLC-UV method.

The *in vitro* drug release study of the three formulations were conducted with Franz cell apparatus. The mSLF was used as dissolution media and 0.45 µm cellulose acetate membrane filter (Sartorius AG, Goettingen, Germany) was applied. Briefly, an accurately weighed amount (10 mg) of spray dried nanoparticles of each formulations were scattered onto the membrane which was previously wetted with the dissolution media for 1 hour. 1 ml of

samples were withdrawn at various time intervals for 5 hours and replaced with fresh dissolution medium. After the measurement, membrane was rinsed with 2 ml of MeOH and the drug content of the possibly remained powders was determined. The sample preparation and the measurement was the same as mentioned above. The cumulative amount of apigenin release over the time was plotted for each formulations. All measurements were performed in triplicate.

2.4.7. Aerosol delivery of BSA-Api formulations

In vitro aerodynamic performance of BSA-Api formulations was assessed using the next generation impactor (NGI; Copley Scientific Ltd., Nottingham, UK), connected sequentially to a low capacity pump via the critical flow controller (Model LCP5; Copley Scientific Ltd., Nottingham, UK). During the measurement the pump was operated at air flow rate of 60 L/min for 4 s. The 3x10 mg powder aliquots from each formulation were loaded manually into gelatine capsules (size 3) and placed into the inhaler device (Cyclohaler®, Pharmachemie, London, UK) which was connected to the NGI via an airtight rubber adaptor and a stainless steel USP throat. The NGI stages were assembled with an induction port, a pre-separator and a filter was placed in the final stage. Prior to the impaction, the collection plates were uniformly coated with 1 ml of 1% silicone oil in N-hexane solution and allowed to dry leaving a thin film of silicone oil on the plate surface in order to prevent the re-entrainment of the particles and the pre-separator was filled with 15 ml DMSO:MeOH (50:50%, v/v) mixture. After the deposition of the powders in the NGI, the amount of each formulation was cumulatively collected onto silicone-coated plates for each of the stages. The inhaler, mouth piece, induction port, pre-separator and the collection plates were rinsed with DMSO:MeOH (50:50%, v/v) mixture, collected in volumetric flasks (10 or 25 ml) and made up to volume. The samples were determined by using HPLC method as described previously. To characterize the aerosol performance the following parameters were calculated based on

the drug mass of each fraction: emitted dose (ED, %): the percentage of the entire dose depositing from the mouthpiece of the inhaler device and recovered dose (RD, %): the total recovered drug mass. The fine particle fraction (FPF, <4.46 μm) is defined as the percentage of the emitted dose which deposited from the Stage 2-7 and the micro orifice-collector (MOC). The mass median aerodynamic diameter (MMAD) and geometric standard deviation (GSD) were calculated from the inverse of the standard normal cumulative mass distribution against the natural logarithm of the effective cut-off diameter of the respective stages. All measurements were carried out in triplicate.

2.4.8. Particle morphology

Morphology of Api powder and spray-died nanoparticles was examined using scanning electron microscopy (SEM) analysis. The dry powder of the formulations was placed on the sample holder using double adhesive tape and gold coating (~20 nm thickness) was applied. Examinations were performed by FEI Inspect^{TM} S50 (Hillsboro, Oregon, USA) scanning electron microscope at 20.00 kV accelerating voltage. Original magnifications were 8000x, 10,000x and 20,000 x with accuracy of ± 2%.

2.5. Antioxidant activity

The antioxidant activities of the prepared spray-dried formulations were compared to the pure Api in order to investigate the effectiveness of the formulation. The free radical scavenging activity was measured by using DPPH$^{\bullet}$ method as described previously[31] with slight modifications. Methanolic stock solution of 0.1 mM DPPH$^{\bullet}$ reagent was freshly prepared and protected from light. Standard curve was plotted between the DPPH$^{\bullet}$ concentration (0.01-0.1 mM) and absorbance, the linear relationship was calculated graphically. 1 ml of MeOH was added to the BSA-Api-NPs and the concentration of Api were the same in each sample for the comparability. Thereafter 2 ml of 0.06 mM DPPH$^{\bullet}$ reagent was added to the samples, vortex mixed for 10 seconds and protected from light. The

absorbance at 517 nm was determined with spectrophotometer (UV-Vis spectrophotometer, Metertech SP-8001, Metertech Inc., Taipei, Taiwan) in every 15 minutes until the steady state (when no further discoloration could be observed). The addition of samples resulted decrease in the absorbance of DPPH˙ due to the scavenging activity of Api. The exact concentration of the free radical was calculated using the standard curve. To calculate the inhibition of the free radical DPPH˙ the following equation (Eq.3.) was used:

$$I\ (\%) = \frac{A_0 - A_S}{A_0} \times 100 \qquad \text{Eq.3.}$$

Where I (%) is the inhibition in percent, A_0 is the absorbance of the DPPH˙ solution and A_s is the absorbance of the sample. All measurements were carried out triplicate and the data were expressed as the mean value ± SD.

3. RESULTS AND DISCUSSION

3.1. Characterization of BSA-Api-NPs

3.1.1. Size, zeta potential and drug content

Albumin is a natural protein that has been widely used as a macromolecular carrier for many drugs with low water solubility. Several techniques are available to prepare albumin nanoparticles including desolvation (coacervation), nab (nanoparticle albumin bound)-technology and self-assembly[14] . In this study the BSA-Api-NPs were prepared by using modified nab-technology with ultrasonication. The achieved mean particle size of three samples was 376 ± 7.824 nm with a polydispersity index of 0.285 ± 0.01. The size of albumin NPs less than 500 nm could localize effectively in the lung. The PDI value indicated narrow particle size distribution and the uniformity of the nanoparticles. The zeta potential was -19.20 ± 0.818 mV. The higher the zeta potential, the more stable the formulation is, less aggregation occurs[32]. The EE was determined to be 82.61 ± 4.56% and the DL was 7.51 ± 0.415%. Therefore these results confirmed the high encapsulation efficiency of apigenin by BSA-NPs and it can be attractive tool in encapsulation flavonoids for delivery. Similar data were found

in the literature when encapsulating flavonoids into albumin nanoparticles. Human serum albumin-bound curcumin nanoparticles resulted 7.2 ± 2.5% loading efficiency[33] and scutellarin-loaded bovine serum albumin nanoparticles possess 64.46% EE and 6.73% DL[34].

3.1.2. Fluorescence spectroscopy

The phenomenon of fluorescence quenching can result from various inter and intramolecular interactions such as energy transfer, conformational changes, complex formation (static quenching) or collisional interaction (dynamic quenching). During static quenching the quencher forms a stable non-fluorescent complex with the fluorophore, however, during dynamic quenching it collides with the fluorophore and facilitates non-radiative transitions to the ground state[35]. Therefore quenching of the intrinsic fluorescence of the two tryptophan residues (Trp-134 and Trp-212) of BSA can offer information about the changes in molecular microenvironment of these fluorophores, located in domain I and II, respectively. Trp-134 residue is located close to the protein surface in a hydrophilic environment, while Trp-212 is within a protein pocket which is hydrophobic (subdomain II A). The Trp-214 in human serum albumin (HSA) is located similarly to Trp-212 in BSA[36-38]. The quenching effect of Api on fluorescence intensity of serum albumins (BSA and HSA) has been studied previously[36, 39-42] but there is no data related to its behavior in a nanoparticulate system. Studies have shown that the increasing concentration of Api resulted in a decrease in the fluorescence emission intensity of serum albumin solutions. This was mainly attributed to complex formation (static quenching), however, it could be dynamic quenching at higher Api concentrations[42]. Nevertheless, all studies concluded that Api most likely binds to the sub-domain IIA of Site I side with electrostatic and hydrophobic interactions, through which H-bonds and non-radiative energy transfer can occur. The binding could affect the conformation of Trp micro-region but the secondary structure of serum albumin is not altered[36, 39, 41].

However, the pH and ionic concentrations (e.g. NaCl) can affect the fluorescence quenching on the binding parameters of apigenin to BSA[43].

Figure 2 demonstrates the fluorescence emission spectra of BSA solution, BSA-NPs and BSA-Api-NPs. The fluorescence intensity of BSA-NPs decreased slightly compared to BSA solution with no obvious shift of the maximum position at 350 nm. It was probably due to the conformational changes of the protein. The significantly lower emission intensity of BSA-Api-NPs indicates that Api could quench the fluorescence of BSA which is also reflected on the 3D projections (**Figure 3**). All of these findings indicate that Api binds to the Trp region (Trp-212, subdomain II A) but the spectral maximum was not affected therefore hydrophobicity and polarity of the fluorophore residues are not altered. It was concluded that Api can be bound to the Trp region of serum albumin nanoparticles similarly to the solutions.

3.2. Characterization of spray-dried BSA-Api-NPs

3.2.1. Determination of residual moisture

Moisture content is mainly influenced by the spray drying conditions. Increased heat energy availability provided by regulating inlet air temperature and aspirator capacity allows more efficient drying, thus resulting in the lower moisture content demonstrated. However, degradation of heat sensitive materials such as proteins may occur; therefore inlet air temperature should be kept below 120 °C[44]. The water content is also affected by the type of excipients and the ratio with the nanoparticles[45]. Moisture content is an important factor that can significantly influence the aerodynamic properties of aerosols. It can change the surface of particles, promote aggregation and influence the crystallinity of the spray-dried samples[44]. In this study, the residual water content was determined by using Karl Fisher titration. All formulations had relatively low moisture content which followed the rank order of L-leucine (4.11 ± 0.21%, w/w) < excipient-free (4.55 ± 0.49%, w/w) < lactose (5.8 ± 0.36%, w/w) containing products. These results demonstrate that the optimized outlet air temperature

(around 65 °C) was suitable for serum albumin. The L-leucine containing formulation had the lowest water content due to the low hygroscopic behavior of this amino acid[46, 47]. The low moisture content can potentially improve the flowability and consequently enhance lung deposition due to reduced aggregation as expected. Storage conditions are also important, e.g. the spray-dried amorphous lactose particles could transform into crystals easily in humidity above 30%[48].

3.2.2. Fourier-Transform Infrared Spectroscopy (FT-IR)

FTIR analysis allows a quick and efficient identification of the compounds and by their functional groups and bond vibrations. In the spectrum of raw Api, the following characteristic regions were observed: 2710-2580 cm^{-1} O-H bond, 1730-1680 cm^{-1} C=O stretch and 1450-1380 cm^{-1} C-H bend. A broad peak observed at 3300 cm^{-1} can be attributed to O-H stretching and those bands at 1600-1400 cm^{-1} (C-C stretch in ring) and 900-675 cm^{-1} (C-H 'oop') can be assigned to the aromatic group (**Figure 4 A**). In the spectrum of BSA protein, the amide I band at 1635 cm^{-1} (mainly C=O stretch) and amide II band at 1530–1500 cm^{-1} (C–N stretching and N–H bend) can be seen. The medium broad peak at 3276 cm^{-1} corresponds to bonded N-H stretch of amide and a smaller band at 1057 cm^{-1} is the C-N stretch of aliphatic amine. In the spectra of the excipients-free formulation, the characteristic amide bands of BSA can be seen and peak at 830 cm^{-1} indicating the presence of Api (aromatic) which is an indirect confirmation of Api encapsulation on BSA-NPs. Conformational changes can be suggested due to the lack of the peak of aliphatic amine.

The spectra of raw Api, BSA, lactose and lactose containing product are displayed on **Figure 4 B**. In the spectra of lactose there is also a broad band around 3300 cm^{-1} indicating the stretching vibration of hydroxyl group. A weak band at 1654 cm^{-1} is the bending vibration of the crystalline water and peaks at 1200-1070 cm^{-1} demonstrate the stretching vibration of C-O-C in the glucose and galactose. The spectrum of amorphous lactose has the less number and

defined peaks and therefore it could be distinguished from the crystalline spectrum[49]. The characteristic broad band at 3300 cm^{-1} in the spectrum of spray-dried product could originate from the residual water content that is further supported by the Karl Fischer titration data (lactose containing product had the highest water content). Similarly to the spectrum of excipients-free formulation, the amide bands of BSA and a small peak of Api could be observed. The peaks at 1200-1070 cm^{-1} demonstrate the lactose content and the amorphous state could be assumed.

Functional groups of L-leucine lead to its characteristic spectrum (**Figure 4 C**). The strong band in the region of 2970-2910 cm^{-1} can be accounted for the aliphatic C-H stretching. The bonded N-H stretch is present in the region of 2600-2450 cm^{-1}. The NH_2 bending and the C-N skeletal vibration appear in the regions of 1595-1550 cm^{-1} and 1250-1020 cm^{-1} [50]. The presence of BSA characteristic peaks on the spray-dried formulation could be mainly observed with and a small peak of Api but the major characteristic peaks of L-leucine are obscured.

3.2.3. X-ray powder diffraction (XRPD)

XRPD is considered to be the most accurate method to study crystalline structure[51]. The combined XRPD diffractograms of Api and spray-dried formulations are presented in **Figure 5**. The characteristic narrow diffraction peaks of Api are due to the crystalline state of the commercially available material. In comparison, broad diffuse peaks could be observed in the diffractograms of the spray-dried formulations suggesting the amorphous state of BSA-Api-NPs. The observed XRD patterns of spray-dried L-leucine and lactose were consistent with literature[48, 52, 53].

3.2.4. Differential scanning calorimetry analysis (DSC)

The DSC curves of raw Api, excipents, physical mixtures and spray-dried formulations were studied to examine crystallinity. As seen in **Figure 6**, there is only one

sharp endothermic peak at 360 °C indicating the melting point of raw Api; no impurities were observed. Drug free albumin exhibited two broad peaks with onset values of 220 °C and 310 °C. The evaporation of residual water occurred at 50-120 °C. The melting point of Api on the thermograms of raw material and physical mixtures corresponds to the crystalline habitus. In the thermograms of physical mixtures on **Figure 6 B** the endothermic peak at 140 °C indicating the crystalline lactose[54] and the sublimation of L-leucine crystals occurred at 200-230 °C (**Figure 6 C**)[55]. However, in each spray-dried formulation the absence of endotherms confirms the loss of crystallinity. No peak could be observed around 360 °C indicating that Api is in amorphous state due to the spray drying process which is in agreement with the XRPD diffractograms. The amorphous form generated may result higher solubility of the powders and dissolution of apigenin in lung fluids.

3.2.5. Aerosol particle size analysis and redispersibility in water

Dry powder formulations of BSA-Api-NPs were prepared with the aim of studying the influence of excipients on the particle size and aerodynamic behavior. The deposition of aerosols is significantly affected by particle size which should be small enough to pass through the upper airways and large enough to avoid exhalation[56]. Gravitational sedimentation is the main driving force for deposition of a nanoparticulate system in the lung due to the formation of aggregates in the micrometer size range. Particle geometry and surface properties also play a significant role in reaching the bronchioles[22,32]. It is well known that particles can be deposited efficiently deeper in the lung if their aerodynamic diameter is in the range of 1-5 µm and only those with 1-3 µm can reach the respiratory zone[57]. Particles, larger than 5 µm tend to deposit in the oropharynx and the mucociliary clearance plays a role in clearing the particles towards the pharynx. However, very small particles, less than 1 µm are usually exhaled because of the low inertia[58, 59]. Mucociliary clearance is the part of the natural defense mechanism of the lung as well as the phagocytosis of macrophages in the alveolar

region. The aerosol particle size was determined by Sympatec HELOS laser diffractometer (**Table 1**). The excipient-free and lactose containing products have similar sizes while spray drying with L-leucine produced the smallest particles (D_{50}= 2.473 µm). In all cases, the particle size could ensure the highest probability of delivery of apigenin into the respiratory zone.

Following the re-dispersion of spray powders formulations in distilled water, the size of the particles was preserved in the nanometer size range: without excipient (358.9 ± 5.3 nm, PDI: 0.315 ± 0.013), lactose (366.1 ± 4.8 nm, PDI: 0.382 ± 0.014) and L-leucine (343.7 ± 2.9, PDI: 0.316 ± 0.011) containing products. The spray drying has no significant effect on the average size of the particles suggesting the deposition of apigenin containing nanoparticles in the lung fluid. Moreover, the excipients did not affect adversely the particle size.

3.2.6. Solubility and Drug release studies of BSA-Api formulations

The solubility of apigenin in nanoparticles was investigated in PBS buffer and mSLF (**Figure 7 A**). The results showed that the solubility was slightly increased in mSLF media (82-98% within 5 minutes), however, it was high in PBS buffer as well (79-95% within 5 minutes). These data indicated that the solubility of apigenin could be highly enhanced by BSA nanoparticles in aqueous medium. Nevertheless, the dispersibility enhancers could play a role in the solubility. In case of excipient free formulation, 91% of the encapsulated apigenin was dissolved in mSLF within 5 minutes. Formulation prepared with lactose increased the solubility rate up to 98%, however, it was slower (82%) when using L-leucine and completed within 2 hours. These results could be attributed to the solubility of the excipients themselves: lactose has very good water solubility, but L-leucine possess a low solubility in water[60].

The apigenin release from the spray dried BSA-Api NPs was investigated with Franz cell apparatus. It is a well known device for the dissolution of semisolid dosage forms and

approved by the USP (United States Pharmacopeia). However, there is no standardized method for inhaled powders, Franz cell could be one of the alternative choices due to simulating the diffusion controlled air-liquid interface of the lung. On the contrary, it has some limitations such as small air bubbles under the contact area of membrane to dissolution medium, wide range of standard deviation or the recovery usually around maximum 90% [61]. Based on the solubility measurements, mSLF was applied. The cumulative dissolution curves of the prepared formulations are shown in **Figure 7 B**. As expected, the dissolution was affected by the co-spray dried excipients. Lactose containing product resulted the fastest and highest apigenin release due to the excellent water solubility. This enhancement of the dissolution is supported by previously published data[62]. In contrast, the dissolution rate was decreased when L-leucine was applied. The coating layer of L-leucine slowed down the dissolution of apigenin which could be well observed in the dissolution curve. The low water solubility of L-leucine is able to hinder the dissolution of the drug which was published previously[60]. These results suggest that the excipients play an important role in the solubility and the dissolution as well.

3.2.7. Aerosol delivery of BSA-Api formulations

Particles can be taken up by alveolar macrophages which influences the therapeutic outcome. Those nanoparticles which are soluble and above 200 nm are able to escape from the macrophages therefore exhibit sustained therapeutic effect[63]. The lung deposition and therefore the efficacy of the inhaled therapeutics are governed by their aerosol properties[56]. Manufacturing respirable nanoparticles could be produced by aggregation in the favorable size range or their incorporation into microparticles (1-5 μm) [26]. Lactose monohydrate is a well-known, traditional carrier for improving the performance of inhaled products; however, it is influenced by physicochemical properties and interaction with the active ingredient[64, 65]. It is the only FDA approved carrier and has also been shown to be a potential excipient for

protein encapsulation[27, 65]. Recently, novel materials such as specific amino acids have been developed for pulmonary formulations[26] and L-leucine is one of the most effective dispersibility enhancer among them[47]. Previous studies proved that 5% (w/w) L-leucine improved the aerosol performance of raw naringin[66] and inclusion up to 15% (w/w) L-leucine resulted higher ED and FPF of powder formulation of gentamicin[46].

In this study *in vitro* aerosol properties of three different dry powders formulations were evaluated using the NGI which is regarded as an optimal instrument for analysis of aerodynamic behavior of aerosol formulations for pulmonary drug delivery[67] according to European and US Pharmacopeias. The obtained data and deposition pattern are presented in **Table 2** and in **Figure 8**. It can be seen that more than 90% of apigenin could be recovered from the NGI which is in the acceptable pharmacopeia range (75-125%). The ED ranged between 91-96% indicating good flowability and high dispersibility of the powders. L-leucine containing formulation had the highest ED as it could improve significantly the flowability of the powders [47, 53]. **Figure 8** shows the amount of Api deposited on the throat, device and stages 1-7 expressed as a percentage of the total amount of recovered powder. All formulation exhibited increased deposition in Stage 2 - 4 indicating enhanced drug delivery to the alveolar regions. As expected, improved aerosol performance and deposition (Stage 3 and 4) could be observed when L-leucine was used an as excipient. The FPF is one of the key parameters in aerosol delivery and should be as high as possible[68]. In this study, the FPF values ranged between 58-66%, suggesting that the particles could be delivered into the peripheral regions. Spray drying of nanoparticles in the presence of L-leucine resulted higher FPF value (66%) due to the improved surface properties and morphology of the particles[65]. In general, MMAD values < 5 μm are for pulmonary lung delivery and between 2-3 μm are optimal for deep lung deposition[56]. In each cases, the calculated mass median aerodynamic diameter (MMAD) data were in agreement with the physical diameter size of the particles measured by laser

diffractometer. The data obtained (< 5 μm) support good dispersibility of the particles into the lower airways and the deep lung. Therefore local delivery to the alveoli could be assured by both excipient-free and lactose formulations generated (MMAD 3.2 μm and 3.1 μm). Moreover, formulation with L-leucine (MMAD 2.1 μm) would be more optimal for deep lung deposition. The size distribution of an aerosol is described best by GSD[69]. Based on the GSD data obtained, the L-leucine containing formulation had the narrowest size distribution (1.8 μm) but that of the others was also in the acceptable range (< 3 μm).

The overall values demonstrate that the particles of each dry powder nanoparticle formulation are in the favorable aerodynamic size range, possess good dispersibility properties and particle deposition. Therefore BSA-NPs is an attractive delivery system for pulmonary drug delivery. We demonstrated that L-leucine improved better the aerosolization properties of BSA-Api-NPs than lactose monohydrate. Therefore it can be concluded that the use of excipients influence the aerosol performance of nanoparticles.

3.2.8. Particle morphology

SEM analysis was conducted to investigate the morphology of the powders (**Figure 9 A** and **B**). It is well known that the morphology of the particles is strongly affected by the solubility of the components and the nature of the excipients[46, 47]. The commercially available Api was a crystalline powder featuring needle-shaped crystals. The excipient-free spray-dried nanoparticles exhibited spherical shape and smooth or wrinkled surface. Particles of lactose containing product had raisin-like surface and some of the particles were larger in accordance with the laser diffraction particle size analysis. Powders prepared with L-leucine comprised small and collapsed particles with strongly corrugated surface. The low aqueous solubility of L-leucine leading to a shell on the surface of the droplet which interfere with the diffusion of water therefore corrugated particles could form. This outcome was consistent with previous observations[46,53,70]. Corrugated surface improves the dispersibility of the dry powder

formulations and enhance respirability due to the reduced interparticulate cohesion (Van der Waals forces) which is beneficial for particles intended for inhalation[71].

3.3. Antioxidant activity

Owing to its reproducibility and comparability, the DPPH˙ assay is an established method for investigating the antioxidant properties of natural compounds. Due to the H-donating ability of the antioxidants, a stable reduced DPPH-H molecule can form. The reaction can be seen visually and the detection can be carried out using UV-Vis spectrophotometer[72, 73]. Previous studies confirmed that Api is able to scavenge the DPPH˙ free radial even in nanoscale delivery formulation[74, 75]. In general, the scavenging activity is influenced by concentration and structural features like hydrogen donating ability, position and the degree of hydroxylation[76, 77]. In order to calculate the exact concentration of remaining DPPH˙ in the samples a calibration curve was plotted with R^2=0.9999. The time required to reach the steady state was estimated to be 120 minutes, and the slow reaction kinetic of Api has been reported[74]. The discoloration of the deep purple DPPH˙ free radical indicate the antioxidant properties of free and encapsulated Api. The inhibition of free radicals by the prepared spray-dried formulations were compared to the empty BSA-NPs, methanolic Api solution and "empty" nanoparticles (**Figure 10**). It can be seen that the free and encapsulated Api have similar scavenging activity, moreover, the spray drying did not result in the loss of scavenging activity. It has been reported that serum albumin is a physiological circulating antioxidant in the body[78] which is confirmed by the inhibition capacity of the empty BSA-NPs observed. Similar results were reported when encapsulating rutin and keampferol[79] or quercetin[17] where the antioxidant activity of the flavonoids are retained by BSA. It can be concluded that the antioxidant activity of Api is preserved, moreover, slightly enhanced by the BSA.

4. CONCLUSION

In this study novel apigenin containing albumin nanoparticles were prepared for inhalation against lung injury caused by oxidative stress. Apigenin was recently classified as a BCS II. drug with prominent antioxidant and anti-inflammatory properties in the lung. The obtained results confirmed that incorporation of apigenin into the biocompatible albumin nanoparticles resulted high encapsulation efficiency therefore it could be an attractive tool for the delivery. Moreover, the spray dried nanoparticles possess good ability to re-disperse in aqueous media and size of the particles was preserved in the nanometer size range. The influence of dispersibility enhancers on the physicochemical properties and *in vitro* pulmonary deposition were investigated and compared to the excipient-free formulation. The obtained *in vitro* pulmonary depositions proved that the developed BSA-NP dry powders are potentially able to carry apigenin deep in the lung, reaching the respiratory zone. The use of novel excipient amino acid L-leucine resulted enhanced aerodynamic properties over the traditional lactose monohydrate, indicating that the nature of the excipients and morphology of the particles play a significant role in the formulation of nanoparticles for pulmonary delivery. In addition, the solubility and dissolution characteristics of apigenin from nanoparticles were determined in mSLF dissolution media, the co-spray dried excipients played an important role. The dissolution rate was increased by the water soluble lactose and decreased by L-leucine, which has low water solubility. Therefore the use of excipients should be taken into consideration, may not required in case of albumin nanoparticles. We further confirmed that the antioxidant activity is retained, thus the potential of albumin nanoparticles as an effective pulmonary delivery system for flavonoids such as apigenin.

ACKNOWLEDGEMENTS

The authors gratefully acknowledge to Róbert Kovács for providing the SEM pictures at Budapest University of Technology and Economics.

Author Disclosure Statement

The authors declare that there are no conflicts of interest.

REFERENCES

1. Chow C-W, Herrera Abreu MT, Suzuki T, and Downey GP. Oxidative Stress and Acute Lung Injury. *Am J Respir Cell Mol Biol*. 2003;29:427-431.
2. Chen XW, Serag ES, Sneed KB, and Zhou SF. Herbal bioactivation, molecular targets and the toxicity relevance. *Chem Biol Interact*. 2011;192:161-176.
3. Patel D, Shukla S, and Gupta S. Apigenin and cancer chemoprevention: progress, potential and promise (review). *Int J Oncol*. 2007;30:233-245.
4. Kim SJ, Jeong HJ, Moon PD, Lee KM, Lee HB, Jung HJ, Jung SK, Rhee HK, Yang DC, Hong SH, and Kim HM. Anti-inflammatory activity of gumiganghwaltang through the inhibition of nuclear factor-kappa B activation in peritoneal macrophages. *Biol Pharm Bull*. 2005;28:233-237.
5. Kowalski J, Samojedny A, Paul M, Pietsz G, and Wilczok T. Effect of apigenin, kaempferol and resveratrol on the expression of interleukin-1beta and tumor necrosis factor-alpha genes in J774.2 macrophages. *Pharmacol Rep*. 2005;57:390-394.
6. Lee J-H, Zhou H, Cho S, Kim Y, Lee Y, and Jeong C. Anti-inflammatory mechanisms of apigenin: inhibition of cyclooxygenase-2 expression, adhesion of monocytes to human umbilical vein endothelial cells, and expression of cellular adhesion molecules. *Archives of Pharmacal Research*. 2007;30:1318-1327.
7. Chen L and Zhao WEI. Apigenin protects against bleomycin-induced lung fibrosis in rats. *Exp Ther Med*. 2016;11:230-234.
8. Luan RL, Meng XX, and Jiang W. Protective Effects of Apigenin Against Paraquat-Induced Acute Lung Injury in Mice. *Inflammation*. 2016; 39:752-758.
9. Basios N, Lampropoulos P, Papalois A, Lambropoulou M, Pitiakoudis MK, Kotini A, Simopoulos C, and Tsaroucha AK. Apigenin Attenuates Inflammation in

Experimentally Induced Acute Pancreatitis-Associated Lung Injury. *J Invest Surg*. 2015;2:1-7.

10. Patil R, Babu RL, Naveen Kumar M, Kiran Kumar KM, Hegde S, Ramesh G, and Chidananda Sharma S. Apigenin inhibits PMA-induced expression of pro-inflammatory cytokines and AP-1 factors in A549 cells. *Mol Cell Biochem*. 2015;403:95-106.

11. Wang J, Liu Y-T, Xiao L, Zhu L, Wang Q, and Yan T. Anti-Inflammatory Effects of Apigenin in Lipopolysaccharide-Induced Inflammatory in Acute Lung Injury by Suppressing COX-2 and NF-kB Pathway. *Inflammation*. 2014;37:2085-2090.

12. Zhang J, Liu D, Huang Y, Gao Y, and Qian S. Biopharmaceutics classification and intestinal absorption study of apigenin. *Int J Pharm*. 2012;436:311-317.

13. Ajazuddin and Saraf S. Applications of novel drug delivery system for herbal formulations. *Fitoterapia*. 2010;81:680-689.

14. Elzoghby AO, Samy WM, and Elgindy NA. Albumin-based nanoparticles as potential controlled release drug delivery systems. *J Control Release*. 2012;157:168-182.

15. Hu Y-J, Liu Y, Sun T-Q, Bai A-M, Lü J-Q, and Pi Z-B. Binding of anti-inflammatory drug cromolyn sodium to bovine serum albumin. *Int J Biol Macromolec*. 2006;39:280-285.

16. Fasano M, Curry S, Terreno E, Galliano M, Fanali G, Narciso P, Notari S, and Ascenzi P. The extraordinary ligand binding properties of human serum albumin. *IUBMB Life*. 2005;57:787-796.

17. Fang R, Hao R, Wu X, Li Q, Leng X, and Jing H. Bovine Serum Albumin Nanoparticle Promotes the Stability of Quercetin in Simulated Intestinal Fluid. *J Agr Food Chem*. 2011;59:6292-6298.

18. He X, Xiang N, Zhang J, Zhou J, Fu Y, Gong T, and Zhang Z. Encapsulation of teniposide into albumin nanoparticles with greatly lowered toxicity and enhanced antitumor activity. *Int J Pharm*. 2015;487:250-259.

19. Muralidharan P, Malapit M, Mallory E, Hayes Jr D, and Mansour HM. Inhalable nanoparticulate powders for respiratory delivery. *Nanomedicine: NBM*. 2015;11:1189-1199.

20. Malcolmson RJ and Embleton JK. Dry powder formulations for pulmonary delivery. *Pharm Sci Technol To*. 1998;1:394-398.

21. Stegemann S, Kopp S, Borchard G, Shah VP, Senel S, Dubey R, Urbanetz N, Cittero M, Schoubben A, Hippchen C, Cade D, Fuglsang A, Morais J, Borgström L, Farshi F, Seyfang KH, Hermann R, van de Putte A, Klebovich I, and Hincal A. Developing and advancing dry powder inhalation towards enhanced therapeutics. *Eur J Pharm Sci.* 2013;48:181-194.

22. Yang W, Peters JI, and Williams Iii RO. Inhaled nanoparticles—A current review. *Int J Pharm*. 2008;356:239-247.

23. Geiser M. Update on macrophage clearance of inhaled micro- and nanoparticles. *J Aerosol Med Pulm Drug Deliv*. 2010;23:207-217.

24. Woods A, Patel A, Spina D, Riffo-Vasquez Y, Babin-Morgan A, de Rosales RT, Sunassee K, Clark S, Collins H, Bruce K, Dailey LA, and Forbes B. In vivo biocompatibility, clearance, and biodistribution of albumin vehicles for pulmonary drug delivery. *J Control Release*. 2015;210:1-9.

25. Swarbrick J. *Encyclopedia of Pharmaceutical Technology*. Informa Healthcare:London; 2007; 671 - 1434.

26. Mansour HM, Rhee YS, and Wu X. Nanomedicine in pulmonary delivery. *Int J Nanomedicine*. 2009;4:299-319.

27. Shoyele SA and Cawthorne S. Particle engineering techniques for inhaled biopharmaceuticals. *Adv Drug Deliv Rev*. 2006;58:1009-1029.

28. Sung JC, Pulliam BL, and Edwards DA. Nanoparticles for drug delivery to the lungs. *Trends Biotechnol*. 2007;25:563-570.

29. Desai NP, Tao C, Yang A, Louie L, Yao Z, Soon-Shiong P, and Magdassi S. Protein stabilized pharmacologically active agents, methods for the preparation thereof and methods for the use thereof. Google Patents, 2004. US6749868 B1

30. Son YJ, McConville JT. Development of a standardized dissolution test method for inhaled pharmaceutical formulations. *Int J Pharm*. 2009;382:15–22.

31. Hatano T. KH, Yasuhara T., Okuda T. 2 new flavonoids and other constituents in licorice root-their relative astringency and radical scavenging effects. *Chem Pharm Bull*. 1988;36:2090-2097.

32. Paranjpe M and Muller-Goymann CC. Nanoparticle-mediated pulmonary drug delivery: a review. *Int J Mol Sci*. 2014;15:5852-5873.

33. Kim TH, Jiang HH, Youn YS, Park CW, Tak KK, Lee S, Kim H, Jon S, Chen X, and Lee KC. Preparation and characterization of water-soluble albumin-bound curcumin nanoparticles with improved antitumor activity. *Int J Pharm*. 2011;403:285-291.

34. Wei Y, Li L, Xi Y, Qian S, Gao Y, and Zhang J. Sustained release and enhanced bioavailability of injectable scutellarin-loaded bovine serum albumin nanoparticles. *Int J Pharm*. 2014;476:142-148.

35. Valeur B. *Molecular fluorescence principles and applications*. Wiley-VCH: Weinheim; 2002; 73-124.

36. Yuan J-L, lv Z, Liu Z-G, Hu Z, and Zou G-L. Study on interaction between apigenin and human serum albumin by spectroscopy and molecular modeling. *J Photochem Photobiol A*. 2007;191:104-113.

37. Naveenraj S and Anandan S. Binding of serum albumins with bioactive substances – Nanoparticles to drugs. *J Photochem Photobiol C*. 2013;14:53-71.

38. Tayeh N, Rungassamy T, and Albani JR. Fluorescence spectral resolution of tryptophan residues in bovine and human serum albumins. *J Pharm Biomed Anal*. 2009;50:107-116.

39. Zhao X-N, Liu Y, Niu L-Y, and Zhao C-P. Spectroscopic studies on the interaction of bovine serum albumin with surfactants and apigenin. *Spectrochim Acta A Mol Biomol Spectrosc*. 2012;94:357-364.

40. Lin C-Z, Hu M, Wu A-Z, and Zhu C-C. Investigation on the differences of four flavonoids with similar structure binding to human serum albumin. *J Pharm Anal*. 2014;4:392-398.

41. Cao H, Liu Q, Shi J, Xiao J, and Xu M. Comparing the Affinities of Flavonoid Isomers with Protein by Fluorescence Spectroscopy. *Anal Lett*. 2008;41:521-532.

42. Shang Y and Li H. Studies of the interaction between apigenin and bovine serum albumin by spectroscopic methods. *Russ J Gen Chem*. 2010;80:1710-1717.

43. Tang L, Jia W, and Zhang D. The effects of experimental conditions of fluorescence quenching on the binding parameters of apigenin to bovine serum albumin by response surface methods. *Luminescence*. 2014;29:344-351.

44. Stahl K, Claesson M, Lilliehorn P, Linden H, and Backstrom K. The effect of process variables on the degradation and physical properties of spray dried insulin intended for inhalation. *Int J Pharm*. 2002;233:227-237.

45. Jensen DM, Cun D, Maltesen MJ, Frokjaer S, Nielsen HM, and Foged C. Spray drying of siRNA-containing PLGA nanoparticles intended for inhalation. *J Control Release*. 2010;142:138-145.

46. Aquino RP, Prota L, Auriemma G, Santoro A, Mencherini T, Colombo G, and Russo P. Dry powder inhalers of gentamicin and leucine: formulation parameters, aerosol performance and in vitro toxicity on CuFi1 cells. *Int J Pharm*. 2012;426:100-107.

47. Yang X-F, Xu Y, Qu D-S, and Li H-Y. The influence of amino acids on aztreonam spray-dried powders for inhalation. *Asian J Pharm Sci*. 2015;10:541-548.

48. Wu L, Miao X, Shan Z, Huang Y, Li L, Pan X, Yao Q, Li G, and Wu C. Studies on the spray dried lactose as carrier for dry powder inhalation. *Asian J Pharm Sci*. 2014;9:336-341.

49. Listiohadi Y, Hourigan J, Sleigh R, and Steele R. Thermal analysis of amorphous lactose and α-lactose monohydrate. *Dairy Sci Technol*. 2009;89:43-67.

50. Němec I and Mička Z. FTIR and FT Raman study of L-leucine addition compound with nitric acid. *J Mol Struct*. 1999;482–483:23-28.

51. Newman AW and Byrn SR. Solid-state analysis of the active pharmaceutical ingredient in drug products. *Drug Discov Today*. 2003;8:898-905.

52. Sou T, Kaminskas LM, Nguyen T-H, Carlberg R, McIntosh MP, and Morton DAV. The effect of amino acid excipients on morphology and solid-state properties of multi-component spray-dried formulations for pulmonary delivery of biomacromolecules. *Eur J Pharm Biopharm*. 2013;83:234-243.

53. Mangal S, Meiser F, Tan G, Gengenbach T, Denman J, Rowles MR, Larson I, and Morton DAV. Relationship between surface concentration of l-leucine and bulk powder properties in spray dried formulations. *Eur J Pharm Biopharm*. 2015;94:160-169.

54. Gombás Á, Szabó-Révész P, Kata M, Regdon G, Jr., and Erős I. Quantitative Determination of Crystallinity of α-Lactose Monohydrate by DSC. *J Therm Anal Calorim.* 2002;68:503-510.

55. Raula J, Seppälä J, Malm J, Karppinen M, and Kauppinen EI. Structure and Dissolution of l-Leucine-Coated Salbutamol Sulphate Aerosol Particles. *AAPS PharmSciTech*. 2012;13:707-712.

56. Yang MY, Chan JGY, and Chan H-K. Pulmonary drug delivery by powder aerosols. *J Control Release*. 2014;193:228-240.

57. Chow AL, Tong HY, Chattopadhyay P, and Shekunov B. Particle Engineering for Pulmonary Drug Delivery. *Pharm Res*. 2007;24:411-437.

58. Liang Z, Ni R, Zhou J, and Mao S. Recent advances in controlled pulmonary drug delivery. *Drug Discov To*. 2015;20:380-389.

59. Heyder J, Gebhart J, Rudolf G, Schiller CF, and Stahlhofen W. Deposition of particles in the human respiratory tract in the size range 0.005–15 μm. *J Aerosol Sci*. 1986;17:811-825.

60. Raula J, Seppälä J, Malm J, Karppinen M, Kauppinen EI. Structure and dissolution of L-leucine-coated salbutamol sulphate aerosol particles. *AAPS PharmSciTech*. 2012; 13:707-12.

61. May S, Jensen B, Wolkenhauer M, Schneider M, Lehr CM. Dissolution techniques for in vitro testing of dry powders for inhalation. *Pharm Res*. 2012;29:2157-66.

62. Knieke C, Azad MA, To D, Bilgili E, Davé RN. Sub-100 micron fast dissolving nanocomposite drug powders. *Powder Technol*. 2015;271:49–60.

63. Patel B, Gupta N, and Ahsan F. Particle engineering to enhance or lessen particle uptake by alveolar macrophages and to influence the therapeutic outcome. *Eur J Pharm Biopharm*. 2015;89:163-174.

64. Kou X, Chan LW, Steckel H, and Heng PWS. Physico-chemical aspects of lactose for inhalation. *Adv Drug Deliv Rev*. 2012;64:220-232.

65. Pilcer G, Wauthoz N, and Amighi K. Lactose characteristics and the generation of the aerosol. *Adv Drug Deliv Rev*. 2012;64:233-256.

66. Prota L, Santoro A, Bifulco M, Aquino RP, Mencherini T, and Russo P. Leucine enhances aerosol performance of Naringin dry powder and its activity on cystic fibrosis airway epithelial cells. *Int J Pharm*. 2011;412:8-19.

67. Taki M, Marriott C, Zeng X-M, and Martin GP. Aerodynamic deposition of combination dry powder inhaler formulations in vitro: A comparison of three impactors. *Int J Pharm*. 2010;388:40-51.

68. Davis SS. Delivery of peptide and non-peptide drugs through the respiratory tract. *Pharm Sci Techn To*. 1999;2:450-456.

69. Musante CJ, Schroeter JD, Rosati JA, Crowder TM, Hickey AJ, and Martonen TB. Factors affecting the deposition of inhaled porous drug particles. *J Pharm Sci*. 2002;91:1590-1600.

70. Lechuga-Ballesteros D, Charan C, Stults CL, Stevenson CL, Miller DP, Vehring R, Tep V, and Kuo MC. Trileucine improves aerosol performance and stability of spray-dried powders for inhalation. *J Pharm Sci*. 2008;97:287-302.

71. Chew NY and Chan HK. The role of particle properties in pharmaceutical powder inhalation formulations. *J Aerosol Med*. 2002;15:325-330.

72. Brand-Williams W, Cuvelier ME, and Berset C. Use of a free radical method to evaluate antioxidant activity. *LWT - Food Science and Technology*. 1995;28:25-30.

73. Villaño D, Fernández-Pachón MS, Moyá ML, Troncoso AM, and García-Parrilla MC. Radical scavenging ability of polyphenolic compounds towards DPPH˙ free radical. *Talanta*. 2007;71:230-235.

74. Al Shaal L, Shegokar R, and Muller RH. Production and characterization of antioxidant apigenin nanocrystals as a novel UV skin protective formulation. *Int J Pharm*. 2011;420:133-140.

75. Papay Z.E AI. Study on the antioxidant activity during the formulation of biological active ingredient. *European Scientific Journal*. 2014;Special Edition 3:252-257.

76. Yang J, Guo J, and Yuan J. In vitro antioxidant properties of rutin. *LWT - Food Science and Technology*. 2008;41:1060-1066.

77. Natella F, Nardini M, Di Felice M, and Scaccini C. Benzoic and Cinnamic Acid Derivatives as Antioxidants: Structure−Activity Relation. *J Agr Food Chem*. 1999;47:1453-1459.

78. Roche M, Rondeau P, Singh NR, Tarnus E, and Bourdon E. The antioxidant properties of serum albumin. *FEBS Lett*. 2008;582:1783-1787.

79. Fang R, Jing H, Chai Z, Zhao G, Stoll S, Ren F, Liu F, and Leng X. Study of the physicochemical properties of the BSA: flavonoid nanoparticle. *Eur Food Res Technol*. 2011;233:275-283.

TABLES

Table 1

Aerosol particle sizes of spray-dried nanoparticles with Sympatec HELOS laser diffractometer in µm.

	Excipient-free	Lactose	L-leucine
ED (%)	91.862 ± 2.735	93.950 ± 1.046	95.183 ± 0.667
FPF (%)	65.617 ± 3.422	58.463 ± 6.031	66.090 ± 2.777
MMAD (µm)	3.210 ± 0.069	3.130 ± 0.001	2.123 ± 0.098
GSD (µm)	2.823 ± 0.113	2.270 ± 0.212	1.887 ± 0.063
RD (%)	99.1 ± 5.012	94.7 ± 4.091	96.3 ± 2.161

Table 2

Aerodynamic characteristic of spray-dried nanoparticles.

	Excipient-free	Lactose	L-leucine
D_{10}	1.033 ± 0.032	1.020 ± 0.070	0.843 ± 0.680
D_{50}	3.030 ± 0.092	3.107 ± 0.102	2.473 ± 0.300
D_{90}	7.110 ± 0.306	7.117 ± 0.337	5.287 ± 0.670

FIGURE CAPTIONS

Figure 1. Molecular structure of apigenin.

Figure 2. Fluorescence emission spectra of BSA solution, BSA nanoparticles and BSA-Api nanoparticles. The excitation wavelength was set to 285 nm (EM: emission, EXC: excitation)

Figure 3. Three dimensional fluorescence emission maps and two dimensional contour maps of empty BSA nanoparticles and BSA-Api nanoparticles. Color scale displays the range of observed fluorescence intensities.

Figure 4. **A)** FT-IR spectra of apigenin (1), BSA (2) and the excipient-free spray-dried BSA-Api nanoparticles (3).

B) FT-IR spectra of apigenin (1), BSA (2), lactose (3) and the spray-dried BSA-Api nanoparticles with lactose (4).

C) FT-IR spectra of apigenin (1), BSA (2), L-leucine (3) and the spray-dried BSA-Api nanoparticles with L-leucine (4).

Figure 5. XRPD diffraction pattern of raw apigenin and the formulations.

Figure 6. **A)** DSC thermograms of apigenin (1), BSA (2) physical mixture (3) and the excipient-free spray dried BSA-Api nanoparticles (4).

B) DSC spectra of apigenin (1), BSA (2), physical mixture (3) and the spray-dried BSA-Api nanoparticles with lactose (4).

C) DSC spectra of apigenin (1), BSA (2), physical mixture (3) and the spray-dried BSA-Api nanoparticles with L-leucine (4).

Figure 7. **A)** Solubility of spray dried BSA-Api formulations in PBS buffer and modified simulated lung fluid (mSLF).

B) Dissolution of apigenin from the formulations as a function of time in modified simulated lung fluid (mSLF).

Figure 8. NGI deposition pattern of the spray dried BSA-Api formulations.

Figure 9. SEM images of raw apigenin (1), excipient-free spray dried BSA-Api nanoparticles (2), spray-dried BSA-Api nanoparticles with lactose (3), spray-dried BSA-Api nanoparticles with L-leucine (4) 20000 x magnification.

Figure 10. Radical scavenging activity of Apigenin solution, empty BSA nanoparticles, BSA-Apigenin nanoparticles (NP) and spray-dried nanoparticles (SD) with excipients. The antioxidant activity is expressed as the inhibition of DPPH˙ free radical in percent.

To whom correspondence should be addressed:

antal.istvan@pharma.semmelweis-univ.hu

Department of Pharmaceutics

Semmelweis University

Hőgyes E. Street 7-9,

H-1092 Budapest, Hungary

Tel/Fax: +3612017-0914; Tel.: +361476-3600/53066, 53087

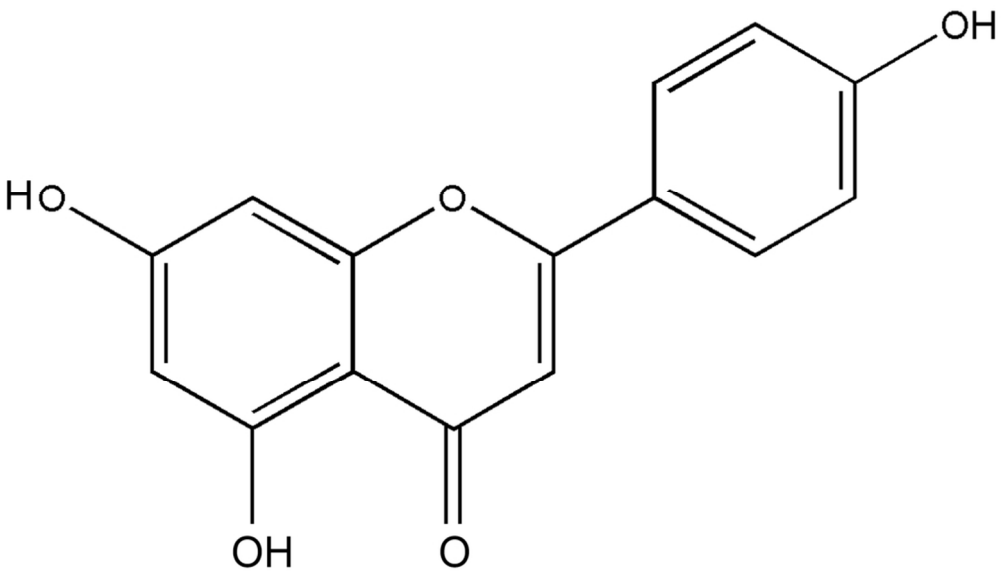

Molecular structure of apigenin.

45x25mm (600 x 600 DPI)

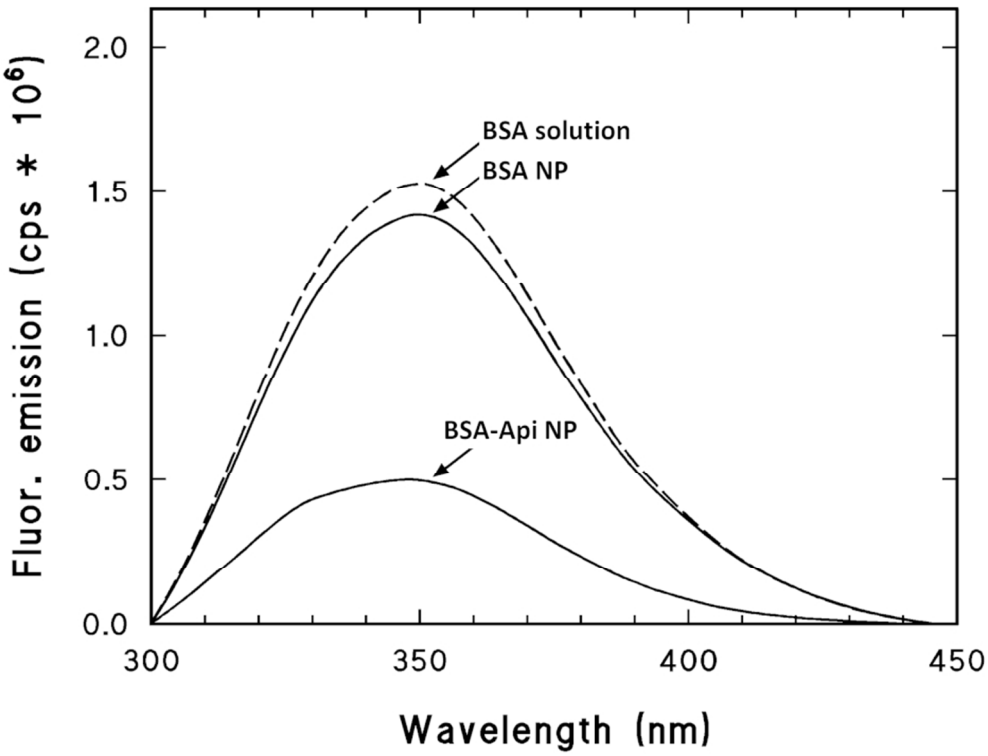

Fluorescence emission spectra of BSA solution, BSA nanoparticles and BSA-Api nanoparticles. The excitation wavelength was set to 285 nm (EM: emission, EXC: excitation)

80x60mm (300 x 300 DPI)

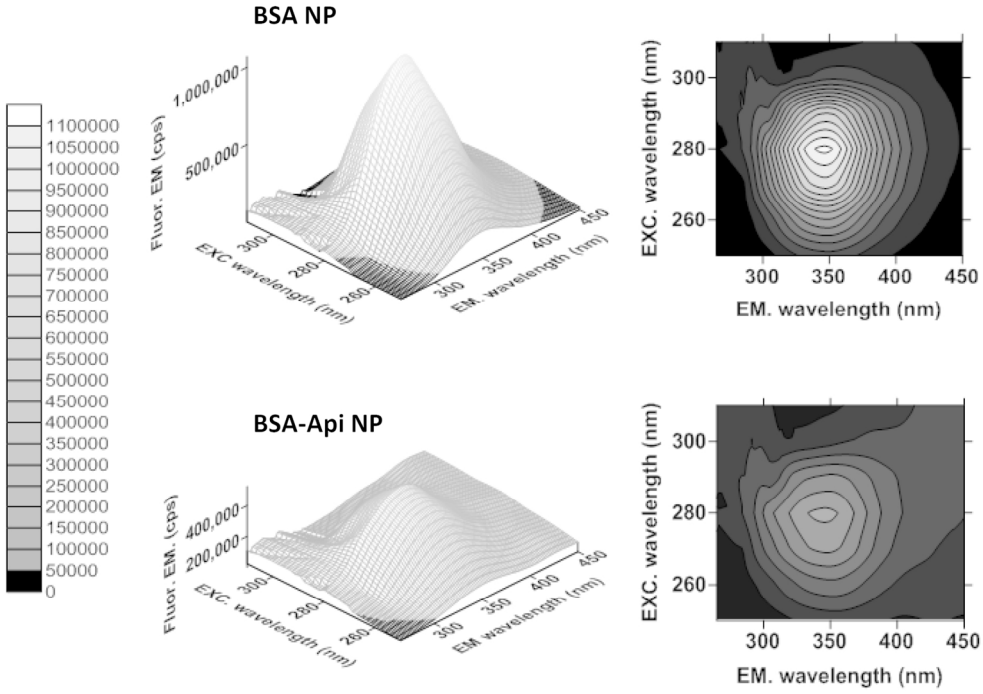

Three dimensional fluorescence emission maps and two dimensional contour maps of empty BSA nanoparticles and BSA-Api nanoparticles. Color scale displays the range of observed fluorescence intensities.

160x110mm (300 x 300 DPI)

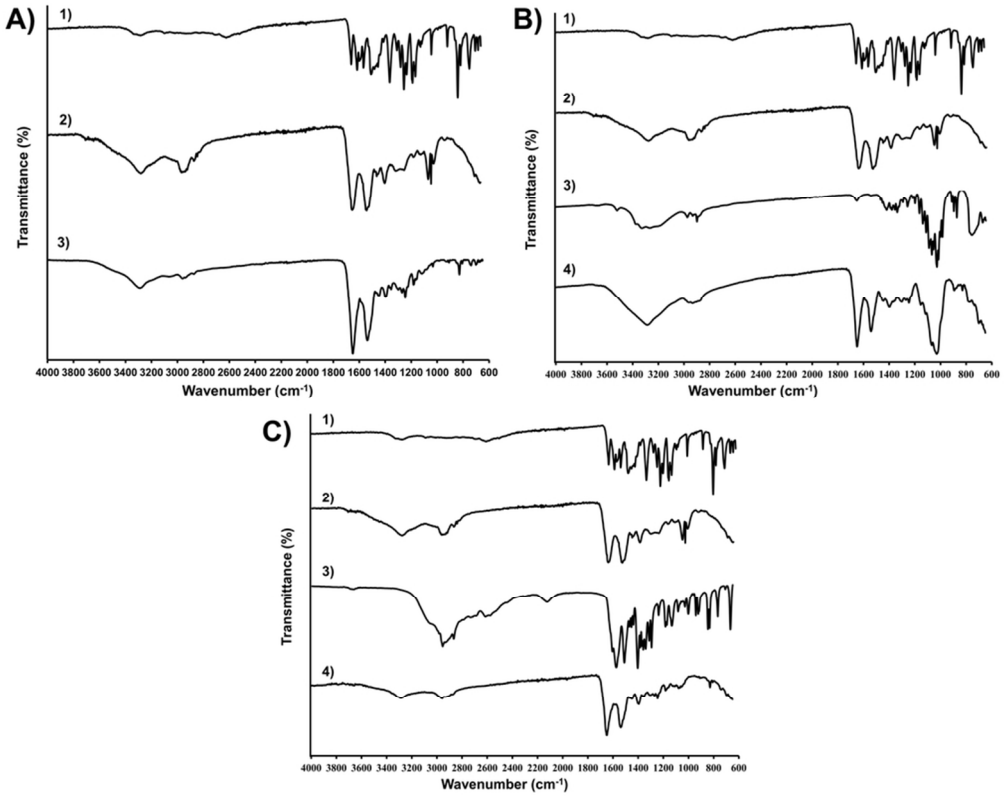

A) FT-IR spectra of apigenin (1), BSA (2) and the excipient-free spray-dried BSA-Api nanoparticles (3).
B) FT-IR spectra of apigenin (1), BSA (2), Lactohale® (3) and the spray-dried BSA-Api nanoparticles with Lactohale® (4).
C) FT-IR spectra of apigenin (1), BSA (2), L-leucine (3) and the spray-dried BSA-Api nanoparticles with L-leucine (4).

42x34mm (600 x 600 DPI)

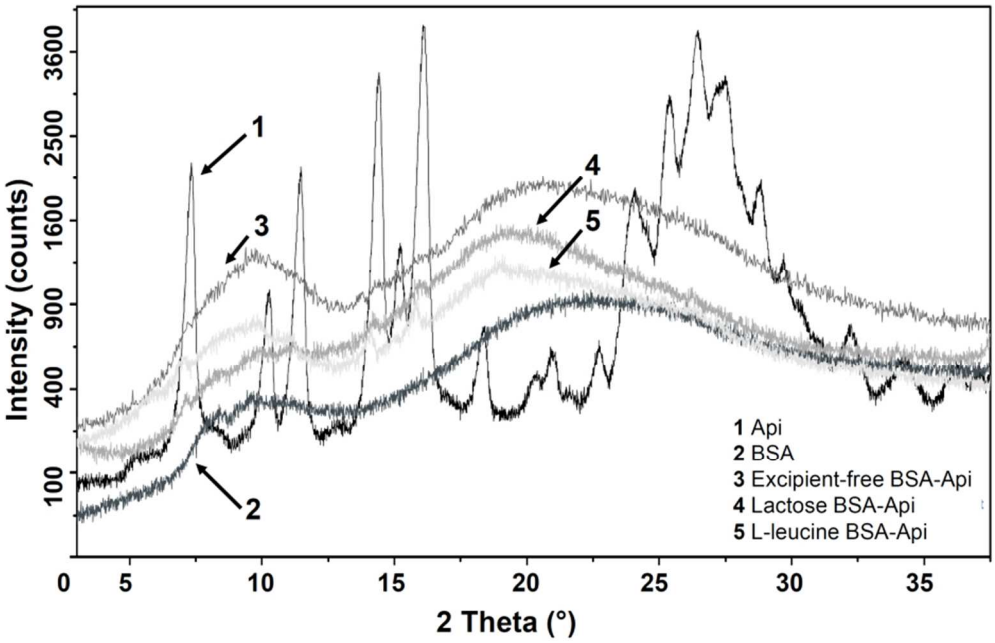

XRPD diffraction pattern of raw apigenin and the formulations.

80x52mm (300 x 300 DPI)

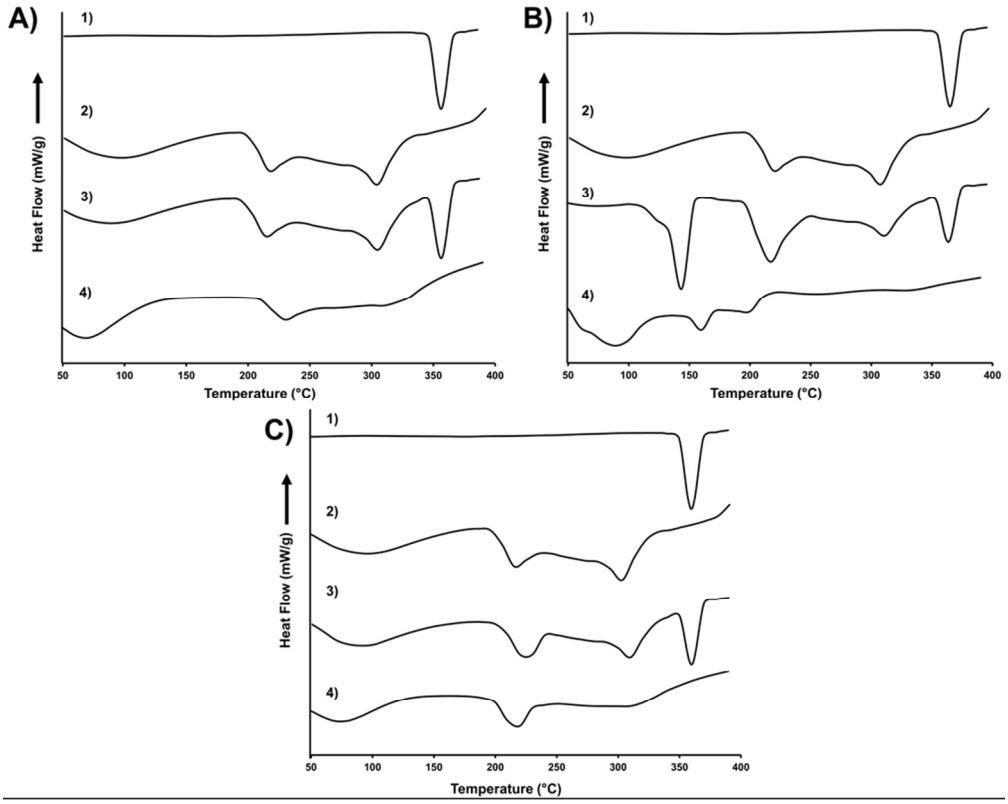

A) DSC thermograms of apigenin (1), BSA (2) physical mixture (3) and the excipient-free spray dried BSA-Api nanoparticles (4).
B) DSC spectra of apigenin (1), BSA (2), physical mixture (3) and the spray-dried BSA-Api nanoparticles with Lactohale® (4).
C) DSC spectra of apigenin (1), BSA (2), physical mixture (3) and the spray-dried BSA-Api nanoparticles with L-leucine (4).

42x34mm (600 x 600 DPI)

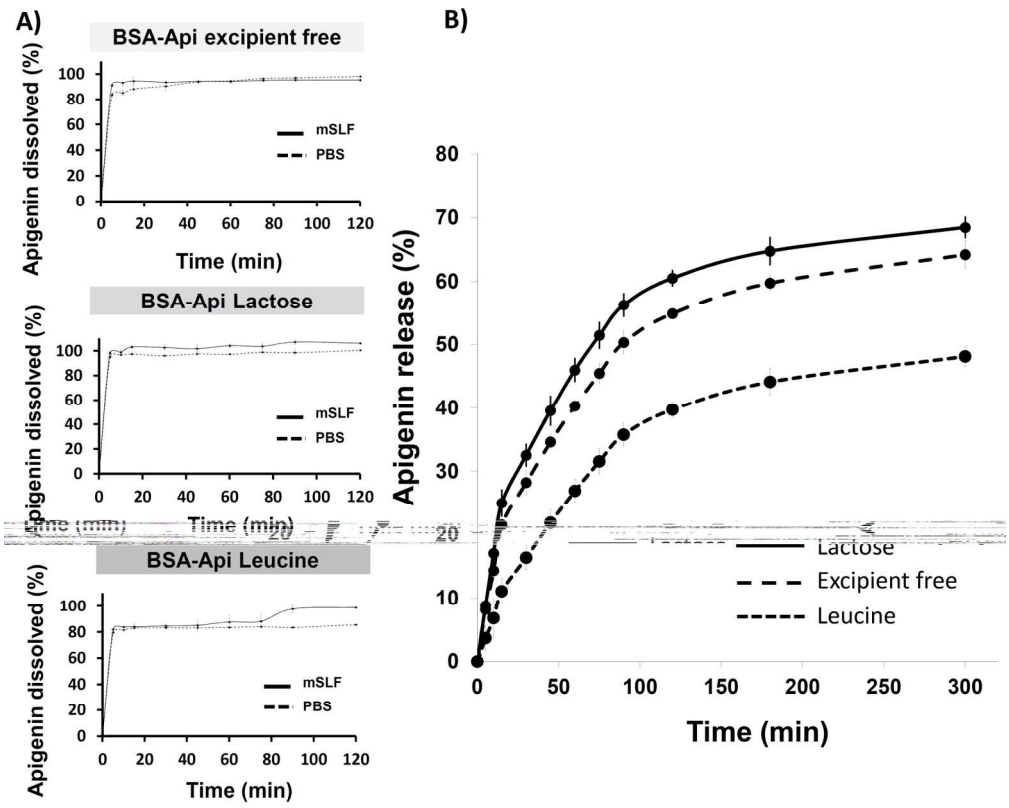

A) Solubility of spray dried BSA-Api formulations in PBS buffer and modified simulated lung fluid (mSLF). B) Dissolution of apigenin from the formulations as a function of time in modified simulated lung fluid (mSLF).

160x128mm (300 x 300 DPI)

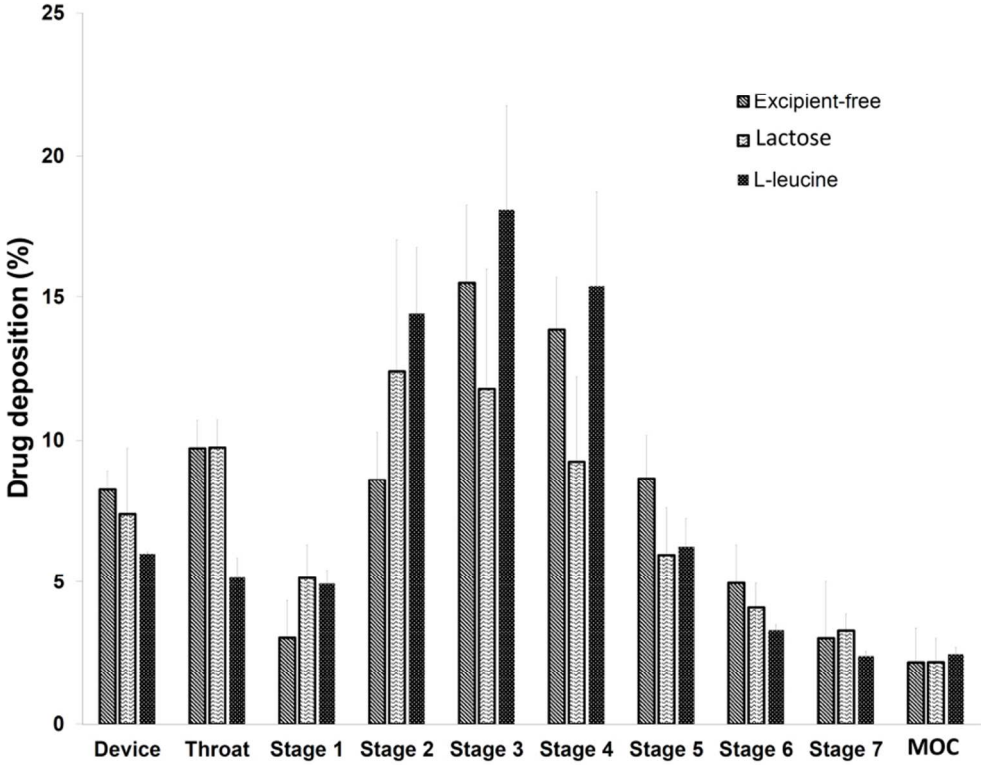

NGI deposition pattern of the spray dried BSA-Api formulations.

80x61mm (300 x 300 DPI)

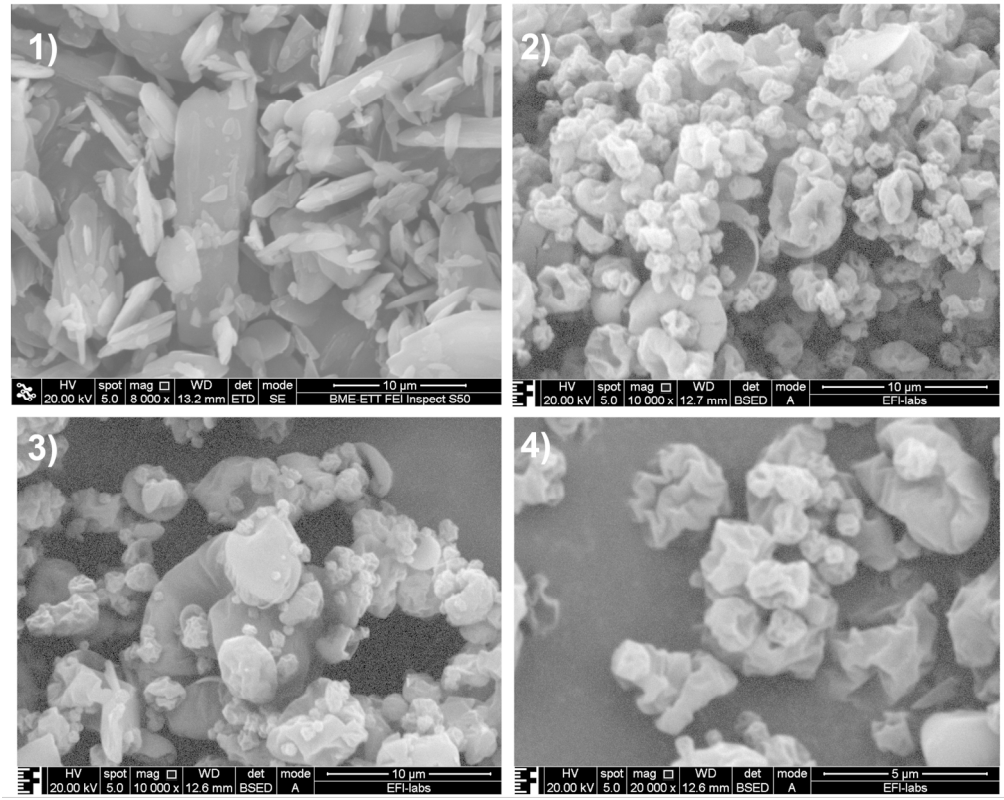

SEM images of raw apigenin (1), excipient-free spray dried BSA-Api nanoparticles (2), spray-dried BSA-Api nanoparticles with lactose (3), spray-dried BSA-Api nanoparticles with L-leucine (4) 20000 x magnification.

160x127mm (300 x 300 DPI)

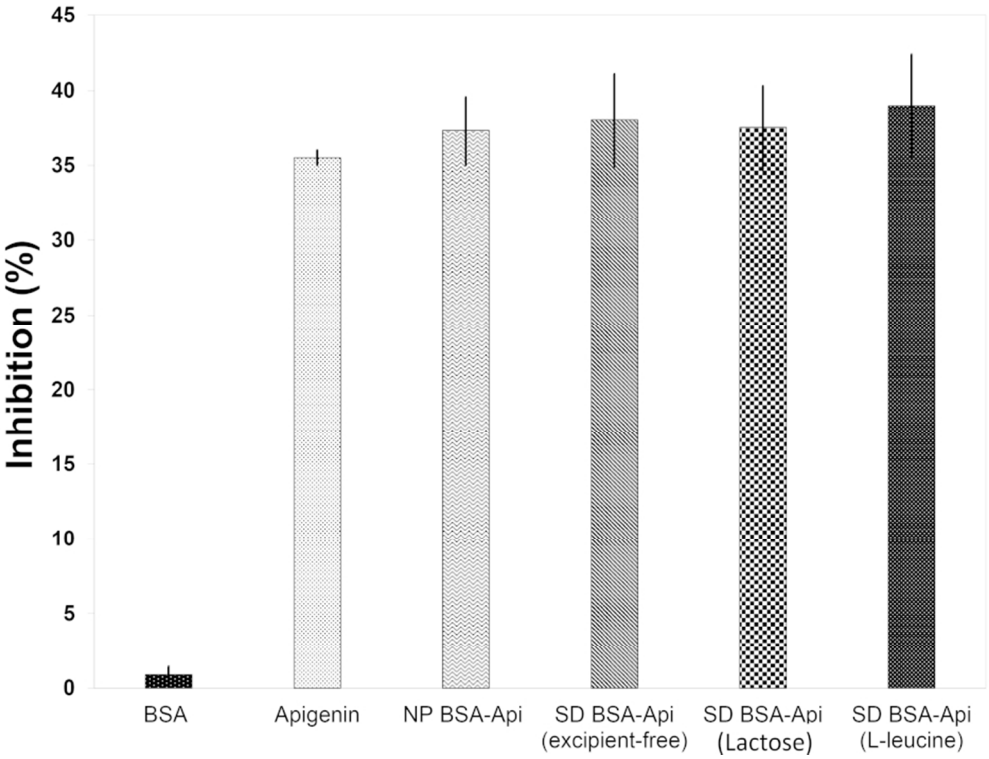

Radical scavenging activity of Apigenin solution, empty BSA nanoparticles, BSA-Apigenin nanoparticles (NP) and spray-dried nanoparticles (SD) with excipients. The antioxidant activity is expressed as the inhibition of DPPH˙ free radical in percent.

80x60mm (300 x 300 DPI)